NONLINEAR PROBLEMS IN EARTHQUAKE ENGINEERING

Mihailo D. Tifunac
University of Southern California, Los Angeles, California 90089
Department of Civil Engineering

Article Outline

Glossary

Meta-stability of man-made structures is the consequence of their upright construction above ground. For excessive dynamic (earthquake) loads, when the lateral deflection exceeds some critical value (this is normally accompanied by softening nonlinear behavior of the structural members), the overturning moment of the gravity forces becomes larger than the restoring moment, and the structure becomes unstable and moves exponentially toward collapse.

Complex and evolving structural systems are structures with a large number of degrees of freedom and many structural members, which for given loads experience softening nonlinear deformations. During strong excitation, continuous changes (typically decreases) in effective stiffness and time-dependent changes in boundary conditions result in a system whose properties are changing with time.

Soil-structure interaction is a process in which the soil and the structure contribute to mutual deformations while undergoing dynamic response. In time, with continuously changing contact area between the foundation and the soil (opening and closing of gaps), when the deformations are large, soil-structure interaction is characterized by nonlinear geometry and nonlinear material properties in both the soil and in the structure.

I. Definition of the Subject

Nonlinear problems in structural earthquake engineering deal with the dynamic response of meta-stable, man-made buildings subjected to strong earthquake shaking. During earthquakes, structures constructed on soft sediments and soils deform together with the underlying soil in the dynamic process called soil-structure interaction. Strong shaking forces the soil-structure systems to evolve through different levels of nonlinear response, with continuously changing properties that depend upon the time history of excitation and on the progression and degree of damage. Thus far, the analyses of this response have used the vibrational approach and lumped mass discrete models to represent real structures. Loss of life and property, however, continue to be high during strong shaking in the vicinity of the faults responsible for earthquakes. This calls for new, more physically refined methods of analysis, which can be based on nonlinear wave propagation, and for balancing of the structural capacities with the power carried by the earthquake waves.

After a brief discussion of the literature on the complex and chaotic dynamics of simple mechanical oscillators, the dynamic characteristics and governing equations in the meta-stable structural dynamics of earthquake engineering are introduced. The nature of the solutions of the governing equations in terms of both the vibrational and the wave representations is discussed, and the dynamic instability, material and geometric nonlinearities, and complexities of the governing equations associated with nonlinear soil-structure interaction are described. Collectively, the examples presented reflect the complex physical nature of meta-stable structural systems that experience nonlinear dynamic response, the characteristics of which change and evolve during earthquake excitation.

II. Introduction

Earthquake engineering, through a cooperation of structural and geotechnical engineers with seismologists and geologists, aims to develop methods for safer design of man-made structures to withstand shaking near intermediate and large earthquakes. This requires addressing the problems of predictability of the response of complicated nonlinear systems, which is one of the important subjects of modern nonlinear science. Through the studies of the dynamic response, earthquake engineers address complex physical problems and issues with important social implications.

The completeness and beauty of the linear differential equations appear to have led to their dominance in the mathematical training of engineers and scientists during most of the 20^{th} century. The recognition that chaotic dynamics is inherent in all nonlinear physical phenomena, which has created a sense of revolution in applied mechanics and physics today, so far has had little if any effect on the research and design of earthquake-resistant structures. In the past, the designs in structural engineering and control systems were kept within the realm of linear system dynamics. However, the needs of modern technology have pushed the design into the nonlinear regimes of large deformations, which has increased the possibility of encountering chaotic dynamic phenomena in structural response. Even a cursory review of papers on chaotic vibrations in mechanical systems leads to the conclusion that chaotic dynamics is not a small, insignificant class of motions and that chaotic oscillations occur in many nonlinear systems and for a wide range of values of the parameters.

If an engineer chooses parameters that produce chaotic output, then he or she loses predictability. However, the chaotic behavior of nonlinear systems does not exclude predictability of the response but rather introduces upper bounds (prediction horizons) (Lighthill 1994) and renders the predictions probabilistic. The important question is then over what time-scale are the forecasts reliable, given the current state and knowledge of the system. Another key ingredient for prediction is an adequate physical model. At present, because of the multitude of interacting phenomena and the absence of physically complete equations of motion, there exists no adequate general model of the complete earthquake response process. While the practical outcome of most work in earthquake engineering remains empirically based, the nonlinear methods are gaining popularity, aiming to decipher the governing phenomena and to assess the reliability of the models. It appears now that the broad-based revolution in the worldview of science that begun in the twentieth century will be associated with chaotic dynamics (Rasband 1990). This revolution should eventually also contribute to better understanding and more complete representation of the response analyses in earthquake engineering.

It has been argued that major changes in science occur not so much when new theories are advanced but when the simple models with which scientists conceptualize a theory are changed (Kuhn 1962). In vibrations, such a conceptual model that embodies the major features of a whole class of problems is the spring-mass system. Lessons emerging from studies of the spring-mass model and several other relevant

models can serve as conceptual starting points for generalizations and also as a guide to further studies of more complex models in earthquake engineering and structural dynamics.

Studies of forced vibrations of a pendulum have revealed complex dynamics and chaotic vibrations (Hackett and Holmes 1985; Gwinn and Westervelt 1985). A simply supported beam with sub-buckling axial compression modeled by a single mode approximation yields a Mathieu type equation and for certain values of the parameters leads to unstable solutions. When nonlinearities are added, these vibrations result in a limit cycle. A related problem is a classical pendulum with a vibrating pivot support, which also leads to chaotic vibrations (Levin and Koch 1981; McLaughlin 1981). Chaotic motions in a double pendulum have been studied by Richter and Scholz (1984), and the complex dynamics and chaotic solutions for a spherical pendulum with two degrees of freedom have been described by Miles (1984a).

Impact-type problems result in explicit difference equations or maps, which can yield chaotic vibrations for certain values of the governing parameters (Lichtenberg and Lieberman 1983). A mass vibrating in a gap between two stiff springs on either side (Holmes 1982; Shaw and Holmes 1983; Shaw 1985) is a simple related model, which suggests a starting points for research in nonlinear vibration of piles, and for impact-type interaction of adjacent buildings, excited by strong earthquake ground motion. The reader can find examples of such problems in the description of damage in Mexico City, for example, during several earthquakes (Lomnitz and Castanos 2006).

Chaotic motions of an elasto-plastic arch have been studied by Poddar et al. (1986). Forced vibrations of a buckled beam, modeled by the Duffing equation, showed that chaotic vibrations are possible (Holmes 1979). Forced vibrations described by a Duffing equation with viscous damping and nonlinear (cubic) elastic (stiffening) spring were studied by Ueda (1980). Fig. 1 summarizes his results and describes the regions of chaotic, periodic (I, II, etc.), and subharmonic (m/n) motions as functions of the damping and forcing amplitudes. This simple equation, representing a hardening spring system, has direct analogues in the dynamics of piles and in the rocking of buildings, both following the strong-motion phase of earthquake shaking after horizontal gaps have been created between the pile (foundation walls) and the soil (Trifunac et al. 2001b).

A mechanical system with a nonlinear restoring force and with a control force added to move the system according to some prescribed signal has been studied by Holmes and Moon (1983) and Holmes (1985). It was shown that such a system exhibits both periodic limit-cycle oscillation and chaotic motions. Chaotic vibrations in continuous beams have been studied for nonlinear body forces and nonlinear boundary conditions (that depend on the motion), and for motions large enough for the nonlinear terms in the equations of motion to be significant (Moon and Holmes 1979; 1985; Moon 1980a,b; Moon and Shaw

1983). Forced planar vibrations of nonlinear elastica (Miles 1984a,b), were shown to become unstable and exhibit chaotic motions under certain conditions.

The above-mentioned studies imply that there is a conflict in the classical engineering description of the world. One aspect of this conflict is the assumption that nature is a deductive system, moving forward in time according to deterministic laws. Another aspect is that a scientist attempting to model portions of the world from finite data projects unverifiable structure onto the local environment. The conflict is that these two views do not match, leaving us with a question: what are models good for? There are many systems in nature that are observed to be chaotic, and for which no adequate physical model exists. Whether a model is adequate or not depends, of course, on the questions asked (Crutchfield 1992). Unfortunately, the art of dynamical modeling is often neglected in discussions of nonlinear and chaotic systems, in spite of its crucial importance (Beltrami 1987). In the following, the modeling problem in earthquake engineering will be illustrated using two common approaches to the solution, one based on an equivalent oscillator and the other one using wave representation.

Stochastic processes have been developed to describe irregular phenomena in deterministic systems that are too complicated or have too many variables to be fully described in detail. For example, stochastic processes have been used to model the response of structures to earthquake and wind forces, which are deterministic, and in principle could be completely described. In practice, the stochastic modeling has been used also as an approximate description of a deterministic system that has unknown initial conditions and may be highly sensitive to the initial conditions. In trying to model real systems, as a result of the modeling process, we sometimes obtain a model that shows very regular behavior, while the real system has very irregular behavior. In that case, random noise is added to the model, but this represents no more than our lack of knowledge of the system structure or the inadequacy of the identification procedure (Kapitaniak 1991).

In earthquake engineering, the complexity of the multi-dimensional real world is reduced to a sub-space, which is defined by (1) the dimensions and properties of the adopted mathematical models, (2) the nature of the adopted boundary conditions, and (3) the method of solution. A linear mechanical system cannot exhibit chaotic vibrations, and for periodic inputs it produces periodic outputs. The chaotic system must have nonlinear elements or properties, which can include, for example, (1) nonlinear elastic or spring elements; (2) nonlinear damping (such as stick-slip friction); (3) backlash, play, or bilinear springs; and (4) nonlinear boundary conditions. The nonlinear effects can be associated with the material properties, with the geometric effects, or both. In the following, the consequences of unorthodox boundary conditions and nonlinear waves in a building will be used to illustrate the extensions and complexities associated with evolving systems. The utility of this complexity can be viewed as the arbiter of the order and randomness.

III. Vibrational Representation of Response

The first modern uses of mechanics in problems of earthquake engineering appeared during the early 1900s, following the earthquake disasters in San Francisco (1906), Messina-Reggio (1908), and Tokyo (1923) and the realization that something needed to be done to prevent such losses of life and property during future events. The first practical steps consisted of introducing the *seismic coefficient* (*shindo* in Japan, and *rapporto sismico* in Italy). This was followed by earthquake-resistant design codes, first adopted in Japan in 1923, and then in California in 1934 (Reitherman 2006). During the same period, there also appeared the first studies of the effects of earthquake shaking on structures in terms of simple mechanical oscillators (Sorrentino 2007), and in the early 1930s the modern theory based on the response spectrum method was introduced (Biot 1932; 1933; 1934). These early developments follow the deterministic formulations of Newtonian mechanics and employ linear models and equations of motion.

III.1. Elementary Vibrational Representation of Response

The basic model employed to describe the response of a simple structure to only horizontal earthquake ground acceleration, $\ddot{\Delta}_x$, is a single-degree-of-freedom system (SDOF) that experiences rocking ψ_r relative to the normal to the ground surface.The model also assumes that the ground does not deform in the vicinity of the foundation—that is, it neglects the soil-structure interaction (Fig. 2). The rotation ψ_r is restrained by a spring with stiffness K_r and by a dashpot with rocking damping constant C_r, providing the fraction of critical damping ς_r. The natural frequency of this system is $\omega_r = \left(K_r / h^2 m_b\right)^{1/2}$, and for small rocking angles it is governed by the linear ordinary differential equation

$$\ddot{\psi}_r + 2\omega_r \varsigma_r \dot{\psi}_r + \omega_r^2 \psi_r = -\ddot{\Delta}_x / h \ . \qquad (1)$$

For any initial conditions, and for arbitrary excitation, this system always leads to a deterministic and predictable response. Eq. (1) was used originally to develop the concept of relative response spectrum and continues to this day as the main vehicle in formulation of most earthquake engineering analyses of response (Trifunac 2003). If the gravity force is considered, ω_r in Eq. (1) has to be reduced (Biot 2006). The system described by Eq. (1) is meta-stable for ψ_r smaller than its critical value. At the critical value of ψ_r, the overturning moment of the gravity force is just balanced by the elastic moment in the restraining spring, and for values greater than the critical value the system becomes unstable.

III.2. Advanced Vibrational Representation of Response

In more advanced vibrational representations of the response, additional components of the earthquake excitation, structural dynamic instability, soil-structure interaction, spatial and temporal variations of the excitation, differential motions at different support points, and nonlinear behavior of the stiffness K_r can be considered, but the structure usually continues to be modeled by mass-less columns, springs, and dashpots, and with a rigid mass m_b. In the following, we illustrate some of the above-mentioned cases.

Dynamic instability. An example of a simple model that includes instability is shown in Fig. 3. It experiences horizontal, vertical, and rocking excitations, which can result, for example, from incident P and SV waves. The structure is represented by an equivalent single-degree-of-freedom system, with a concentrated mass m_b at height h above the foundation. It has a radius of gyration r_b and a moment of inertia $I_b = m_b r_b^2$ about point O. The degree-of-freedom in the model is chosen to correspond to the relative rocking angle ψ_r. This rotation is restrained by a spring with rocking stiffness K_r and by a dashpot with rocking damping C_r (both not shown in Fig. 3), and the gravitational force $m_b g$ is considered. Taking moments about B results in the equation of motion

$$\ddot{\phi}_y + \ddot{\psi}_r + 2\omega_r \varsigma_r \dot{\psi}_r + \omega_r^2 \psi_r = \left\{ -\left(\ddot{\Delta}_x / a \right) \cos\left(\phi_y + \psi_r \right) + \left(\omega_r^2 \varepsilon_g + \ddot{\Delta}_z / a \right) \sin\left(\phi_y + \psi_r \right) \right\} / \varepsilon , \quad (2)$$

where $\varepsilon = h\left(1 + \left(r_b / h\right)^2\right)/a$, $\omega_r^2 = K_r / \left[m\left(h^2 + r_b^2\right) \right]$, ω_r is the natural frequency of rocking, ζ_r is a fraction of critical damping in $2\omega_r \varsigma_r = C_r / \left[m\left(h^2 + r_b^2\right) \right]$, and $\varepsilon_g = 2/\omega_r^2 a$. Eq. (2) is a differential equation coupling the rocking of the foundation, ϕ_y, and of the structure, ψ_r, with the horizontal and vertical motions of the foundation. It is a nonlinear equation the solution to which requires numerical analysis. In this example, we will discuss only the case in which $\phi_y + \psi_r$ is small. Then,

$$\ddot{\psi}_r + 2\omega_r \varsigma_r \dot{\psi}_r + \left\{ \omega_r^2 \left(1 - \varepsilon_g / \varepsilon\right) - \ddot{\Delta}_z / \varepsilon a \right\} \psi_r = -\ddot{\phi}_y + \left\{ -\ddot{\Delta}_x / a + \left(\omega_r^2 \varepsilon_g + \ddot{\Delta}_z / a \right) \phi_y \right\} / \varepsilon . \quad (3)$$

For steady-state excitation by incident P and SV waves with frequency ω, Δ_x, ϕ_y, and Δ_z, and therefore the forcing function of Eq. (3), will be periodic. Equation (3) is then a special form of the Hill's equation. Analysis of the stability of this equation can be found in the work of Lee (1979). For general earthquake excitation, Δ_x, ϕ_y, and Δ_z will be determined by the recorded components of motion, and in predictive analyses by simulated ground motions (Lee and Trifunac 1985; 1987; Wong and Trifunac 1979).

In Eq. (3), ϕ_y describes rocking of the foundation to which the structure is attached. In analyses that do not consider soil-structure interaction, ϕ_y will be determined directly by the rocking component of strong ground motion (Lee and Trifunac 1987; Jalali and Trifunac 2007), and in studies that consider soil-structure interaction ϕ_y will be one of the variables to be determined by the analysis (Lee 1979).

Soil-Structure Interaction. The problem of linear soil-structure interaction embodies the phenomena that result from (1) the presence of an inclusion (foundation, Fig. 4) in the soil (Lee and Trifunac 1982), and (2) the vibration of the structure supported by the foundation, which exerts dynamic forces on the foundation (Lee 1979). Examples and a discussion of the non-linear aspects of soil-structure interaction can be found in Gicev (2005) and in a review of observations of response to earthquake shaking in full-scale structures in Trifunac et al. (2001a,b,c).

The dynamic response of a rigid, embedded foundation to seismic waves can be separated into two parts. The first part corresponds to the determination of the restraining forces due to the motion of the inclusion, usually assumed to be a rigid body. The second part deals with the evaluation of the driving forces due to scattering of the incident waves by the inclusion, which is presumed to be immobile. This can be illustrated by considering a foundation embedded in an elastic medium and supporting an elastic superstructure. The steady-state harmonic motion of the foundation having frequency ω can be described by a vector $\left\{\Delta_x, \Delta_y, \Delta_z, \phi_x, \phi_y, \phi_z\right\}^T$ (Fig. 4), where Δ_x and Δ_y are horizontal translations, Δ_z is vertical translation, ϕ_x and ϕ_y are rotations about horizontal axes, and ϕ_z is torsion about the vertical axis. Using superposition, displacement of the foundation is the sum of two displacements:

$$\{U\} = \{U^*\} + \{U_0\}, \qquad (4)$$

where $\{U^*\}$ is the foundation input motion corresponding to the displacement of the foundation under the action of the incident waves in the absence of external forces, and $\{U_0\}$ is the relative displacement corresponding to the displacement of the foundation under the action of the external forces in the absence of incident wave excitation.

The interaction force $\{F_s\}$ generates the relative displacement $\{U_0\}$, which corresponds to the force that the foundation exerts on the soil and that is related to $\{U_0\}$ by $\{F_s\} = \left[K_s(\omega)\right]\{U_0\}$, where $\left[K_s(\omega)\right]$ is the 6 x 6 complex stiffness matrix of the embedded foundation. It depends upon the material

properties of the soil medium, the characteristics and shape of the foundation, and the frequency of the harmonic motion, and it describes the force-displacement relationship between the rigid foundation and the soil medium.

The driving force of the incident waves is equal to $\{F_s^*\} = [K_s]\{U^*\}$, where the input motion $\{U^*\}$ is measured relative to an inertial frame. The "driving force" is the force that the ground exerts on the foundation when the rigid foundation is kept fixed under the action of the incident waves. It depends upon the properties of the foundation and the soil and on the nature of excitation.

The displacement $\{U\}$ is related to the interaction and driving forces via $[K_s]\{U\} = \{F_s\} + \{F_s^*\}$.

For a rigid foundation having a mass matrix $[M_0]$ and subjected to a periodic external force, $\{F_{ext}\}$, the dynamic equilibrium equation is

$$[M_0]\{\ddot{U}\} = -\{F_s\} + \{F_{ext}\}, \qquad (5)$$

where $\{F_{ext}\} = \{F_{bx}, F_{by}, F_{bz}, M_{bx}, M_{by}, M_{bz}\}$ is the force the structure exerts on the foundation (Fig. 4). Then, Eq. (5) becomes

$$[M_0]\{\ddot{U}\} + [K_s]\{U\} = \{F_s^*\} + \{F_{ext}\}. \qquad (6)$$

The solution of $\{U\}$ requires the determination of the mass matrix, the impedance matrix, the driving forces, and the external forces (Lee 1979).

After the mass matrix $[M_0]$, the stiffness matrix $[K_s]$, and the force $\{F_s^*\}$ have all been evaluated, they can be used to determine the foundation displacement $\{U\}$. For in-plane response excited by P and SV waves, for example, the relative response ψ_r is then given by Eq. (3)

Differential motions. Common use of the response spectrum method (Trifunac 2003) and many dynamic analyses in earthquake engineering implicitly assume that all points of building foundations move synchronously and with the same amplitudes. This, in effect, implies that the wave propagation in the soil is neglected. Unless the structure is long (e.g., a bridge with long spans, a dam, a tunnel) or "stiff" relative to the underlying soil, these simplifications are justified and can lead to a selection of approximate design forces if the effects of soil-foundation interaction in the presence of differential ground motions can be neglected (Bycroft 1980). Simple analyses of two-dimensional models of long buildings suggest that when

$a/\lambda < 10^{-4}$, where a is wave amplitude and λ is the corresponding wavelength, the wave propagation effects on the response of simple structures can be neglected (Todorovska and Trifunac, 1990).

Figure 5 illustrates the "short" waves propagating along the longitudinal axis of a long building or a multiple-span bridge. For simplicity, the incident wave motion has been separated into out-of-plane motion (Fig. 5, top), consisting of SH and Love waves, and in-plane motion (Fig. 5, bottom) consisting of P, SV, and Rayleigh waves. The in-plane motion can further be separated into horizontal (longitudinal), vertical, and rocking components, while out-of-plane motion consists of horizontal motion in the transverse direction and torsion along the vertical axis. Trifunac and Todorovska (1997) analyzed the effects of the horizontal in-plane components of differential motion for buildings with models that are analogous to the sketch in Fig. 5 (bottom), and they showed how the response spectrum method can be modified to include the first-order effects of differential motions. Trifunac and Gicev (2006) showed how to modify the spectra of translational motions, into a spectrum that approximates the total (translational and torsional) responses, and how this approximation is valid for strong motion waves an order of magnitude longer than the structure ($\lambda >> L$).

As can be seen from the above examples the differential motions lead to complex excitation and deformation of the structural members (columns, shear walls, beams, braces), increase the dimensions of the governing differential equations, lead to thee-dimensional dynamic instability problems, and can lead to nonlinear boundary conditions. These are all conditions that create an environment in which, even with the most detailed numerical simulations, it is difficult to predict all of the complexities of the possible responses.

III.3. Nonlinear Vibrational Analyses of Response

For engineering estimation of the maximum nonlinear response of a SDOF system, u_m, in terms of the maximum linear response, u_0, it is customary to specify a relation between u_m and u_0 (Fig. 6). By defining the yield-strength reduction factor as $R_y = u_0 / u_y$, where u_y is the yielding displacement of the SDOF system equivalent spring, and ductility as $\mu = u_m / u_y$, for the same ground motion the ratio u_m / u_0 is then equal to μ / R_y. Veletsos and Newmark (1960,1964) showed that (1) for a long-period SDOF system when its natural period $T_n = 2\pi / \omega_n$ becomes very long, u_m / u_0 tends toward 1 and R_y approaches μ (equal deformation rule); (2) for the response amplitudes governed mainly by the peak excitation velocities, u_m / u_0 can be approximated by $\mu / \sqrt{2\mu - 1}$ and R_y by $\sqrt{2\mu - 1}$ (equal strain energy rule); and (3) for a high-frequency (stiff) system when $T_n \sim 0$, $R_y \sim 1$.

Complexities of simultaneous action of dynamic instability, nonlinearity, and kinematic boundary conditions—example. The model we illustrate next is an SDOF when it is excited by synchronous horizontal ground motion at its two supports (1 and 2 in Fig. 7), but it behaves like a three-degree-of-freedom (3DOF) system when excited by propagating horizontal, vertical, and rocking ground motions. For such a system, the above classical equal energy and equal displacement rules for SDOF system will not apply.

The goals here are to describe the effects of differential motion on strength-reduction factors R_y of the simple structure shown in Figure 7 when it is subjected to all of the components of near-source ground motions, and to illustrate the resulting complexities of nonlinear response. Analyses of the consequences of the differences in ground motion at structural supports, caused by non-uniform soil properties, soil-structure interaction, and lateral spreading, for example, will further contribute to the complexities of the response, but these factors will not be discussed here.

The original response spectrum method was formulated using a vibrational solution of the differential equation of an SDOF system excited by synchronous, and only horizontal (one component), ground motion. The consequences of simultaneous action of all six components of ground motion (three translations and three rotations) on the relative response of an SDOF system are still rarely considered in modern engineering design (Trifunac 2006), even though it has been 75 years since the original response spectrum method was formulated and about 40 years since it became the principal tool in engineering design (Trifunac 2003). Because the response spectrum method has become an essential part of the design process and of the description of how strong motion should be specified for a broad range of design applications (Todorovska et al. 1995), we hope that the present examples will help to further understanding of the complexities of response in more realistic models of structures.

The nature of the relative motion of individual column foundations or of the entire foundation system will depend upon the type of foundation, the characteristics of the soil surrounding the foundation, the type of incident waves, and the direction of wave arrival, with the motion at the base of each column having six degrees of freedom. In the following example, we assume that the effects of soil-structure interaction are negligible; consider only the in-plane horizontal, vertical, and rocking components of the motion of column foundations; and show selected results of the analysis for a structure on only two separate foundations. We assume that the structure is near the fault and that the longitudinal axis of the structure (X axis) coincides with the radial direction (r axis) of the propagation of waves from the earthquake source, so that the displacements at the base of columns are different as a result of the wave passage alone. We suppose that the excitations at the piers have the same amplitude but different phases and that the phase difference (or

time delay) will depend upon the distance between the piers and the horizontal phase velocity of the incident waves.

The simple model we consider, which is described in Fig. 7, represents a one-story structure consisting of a rigid mass, *m*, with length *L*, supported by two rigid, mass-less columns with height *h*, which are connected at the top to the mass and at the bottom to the ground by rotational springs (not shown in Fig.7). The stiffness of the springs, k_ϕ, is assumed to be elastic-plastic, as in Fig. 6, without hardening ($\alpha = 0$). The mass-less columns are connected to the ground and to the rigid mass by rotational dashpots, c_ϕ, providing a fraction of critical damping equal to 5 percent. Rotation of the columns, $\phi_i = \theta_{gi} + \psi_i$ for i = 1,2, which is assumed to be not small, leads us to consider the geometric nonlinearity. The mass is acted upon by the acceleration of gravity, g, and is excited by differential horizontal, vertical, and rocking ground motions, u_{g_i}, v_{g_i}, and $\theta_{g_i}, i = 1,2$ (Fig. 7) at the two bases, so that

$$u_{g_2}(t) = u_{g_1}(t-\tau); \quad v_{g_2}(t) = v_{g_1}(t-\tau); \quad \theta_{g_2}(t) = \theta_{g_1}(t-\tau); \quad \tau = L/C_x,$$

with τ being the time delay between the motions at the two piers and C_x the horizontal phase velocity of the incident waves. The functional forms of u_{g_i}, v_{g_i}, and θ_{g_i} are defined by the near-source ground motions (Jalali and Trifunac 2007),and the rocking component of the ground motion is approximated by (Lee and Trifunac 1987) $\theta_{g_i}(t) = -\dot{v}_{g_i}(t)/C_x$, where $\dot{v}_{g_i}(t)$ is the vertical velocity of the ground motion at the *i-th* column. Of course, in a more accurate modeling, the ratio of the v_{g_i} to u_{g_i} amplitudes will depend upon the incident angle and the character of incident waves, while the associated rocking θ_{g_i} will be described by a superposition of the rocking angles associated with incident body and dispersed surface waves (Lee and Trifunac 1987).

The yield-strength reduction factor for the system subjected to synchronous ground motion is $R_y = f_0 / f_y = u_0 / u_y$, where all of the quantities are defined in Fig. 6. In this example, for the assumed model and because of the differential ground motions and rotation of the beams, the relative rotation for the two columns at their top and bottom will be different. Therefore, it is necessary to define the *R*-factor and ductility for each corner of the system, instead of one factor for the entire system. In all calculations here, we consider the actions of the horizontal, vertical, and rocking components of the ground motion, the effects of gravity force, dynamic instability, and geometric nonlinearity. For the structure in Fig. 7, we calculate maximum linear and nonlinear relative rotations at four corners of the system under downward $(-v_{g_i})$, radial, and rocking, and upward $(+v_{g_i})$, radial and rocking near-source differential ground

motions corresponding to a given earthquake magnitude, ductility μ, and for different time delays, τ. Then we plot R_y versus T_n for the four corners of the system.

Fig. 8 illustrates typical results for R_y versus the oscillator period for near-source, fault-parallel displacement $d_N(t) = A_N(1-e^{-t/\tau_N})/2$ (Jalali and Trifunac 2007), with downward vertical ground displacement, magnitude M = 8, for a ductility ratio of 8 and a time delay of $\tau = 0.05$ s. It shows the results for the top-left, top-right, bottom-left, and bottom-right corners of the system, assuming wave propagation from left to right (see Fig. 7). For reference and easier comparison with the previously published results, we also plot one of the oldest estimates of R_y versus period, using piecewise straight lines (Jalali and Trifunac 2007). The curve $(R_y)_{\min}$ shows the minimum values of R_y for $d_N(t)$ motion with $-v_{g_i}$, and for M = 8, μ = 8, and τ = 0.05 s.

For periods longer than 5 to 10 s, R_y curves approach "collapse boundaries" (Jalali and Trifunac 2007). This is implied in Fig. 8 by the rapid decrease of R_y versus period for periods longer than about 7 s. At or beyond these boundaries, the nonlinear system collapses due to the action of gravity loads and dynamic instability.

The complex results illustrated in Fig. 8 can be simplified by keeping only $(R_y)_{\min}$, since it is only the minimum value of R_y that is needed for engineering design. By mapping $(R_y)_{\min}$ versus period of the oscillator for different earthquake magnitudes, M, different ductilities, μ, and different delay times, τ, design criteria can be formulated for design of simple structures to withstand near-fault differential ground motions (Jalali and Trifunac 2007). Nevertheless, the above shows how complicated the response becomes even for as simple a structure as the one shown by the model in Fig. 7, when differential ground motion with all of the components of motion is considered. In this example, this complexity results from simultaneous consideration of material and geometric nonlinearities, dynamic instability, and kinematic boundary conditions.

IV. Response in Terms of Wave Propagation—An Example

The vibrational representation of the solution of response of a multi-degree-of-freedom system subjected to earthquake shaking is frequently simplified by considering only the fundamental and, occasionally, a few of the lowest frequencies of the system. Doing so is analogous to low-pass filtering of the complete solution (Trifunac 2003; 2005), but it can work well when the excitation amplitudes are small and the

motions are associated with long waves. However, during strong earthquakes, the ground motion contains large displacement pulses, the duration of which can be shorter than the fundamental period of the structure. For this type of excitation, the vibrational representation of response and the response spectrum superposition method cease to be suitable and should be replaced by a solution in terms of propagating waves. For short impulsive ground motions, the damage can occur before the wave entering the structure completes its travel up and down the structure, and well before the wave interference can occur—that is, well before the physical conditions can lead to the interference of waves and creation of the mode shapes.

To illustrate the phenomena that can occur during nonlinear wave propagation in a building, we describe horizontal motions, u, in a one-dimensional shear beam, supported by one-dimensional half space and excited by a vertically propagating shear wave described by a half-sine-pulse (Fig. 9). A finite-difference scheme for solution of this problem with accuracy, $O(\Delta t^2, \Delta x^2)$, where Δx and Δt are the space and time increments, leads to the exact solution for $\beta \Delta t / \Delta x = 1$, where β is the velocity of shear waves. For simplicity, the incident displacement in the soil is chosen to be a sinusoidal pulse with the characteristics shown on Fig. 9.

A mesh with different spatial intervals in the soil and in the building will be used. The equation of motion is

$$v_t = (\sigma)_x / \rho \ , \qquad (7a)$$

and the relation between the derivative of the strain and the velocity is

$$\varepsilon_t = v_x \ , \qquad (7b)$$

where v, ρ, σ, and ε are particle velocity, density, shear stress, and shear strain, respectively, and the subscripts t and x represent derivatives with regard to time and space.

The domain consists of two materials (Fig. 9): (1) $-2\Delta x_s \le x < 0$ with physical properties ρ_s and μ_s, representing foundation soil, and (2) $0 < x \le H_b$ with physical properties ρ_b and μ_b for linear response, where ρ_i is the density and μ_i is the shear modulus in the soil (i = s) or in the building (i = b). $v = \partial u / \partial t$ and $\varepsilon = \partial u / \partial x$ are the velocity and the strain of a particle, and u is out-of-plane displacement of a particle perpendicular to the propagation ray.

It is assumed that the incoming wave is known and that its displacement as a function of time is prescribed at the point 1 in the soil ($x = -2\Delta x_s$). Also, it is assumed that the soil is always in the linear elastic state. The finite difference method for a set of simultaneous equations is used to solve the problem, and spatial intervals are defined by $\Delta x_i = \beta_i \cdot \Delta t$, where β_i is the velocity of shear waves in the soil (i = s) or in the

building (i = b) and Δt is the time step. The transparent boundary adopted for this study, which is described in Fujino and Hakuno (1978), is a perfect, transparent boundary for one-dimensional waves when $\beta \Delta x / \Delta t = 1$. Point 1 is where the prescribed displacement is applied, and we assume that this displacement travels upward in each time step. Point 2 is the boundary point of the model, where the quantities of motion are updated in each time step, and point 3 is the first spatial point, where the motion is computed using finite differences.

For the linear case at the contact (point 3 in Fig. 9), one part of the incoming wave is transmitted into the other medium and one is reflected back into the same medium. The corresponding coefficients are obtained from the boundary conditions of continuity of the displacements and stresses at the contact. For a transmitted wave from medium B to medium A, the transmission coefficient is equal to $k_{trB \to A} = 2 / \left[1 + \rho_a \beta_a / \left(\rho_b \beta_b \right) \right]$. For a reflected wave from medium A back into medium B, this coefficient is $k_{refB \to B} = \left[1 - \rho_a \beta_a / \left(\rho_b \beta_b \right) \right] / \left[1 + \rho_a \beta_a / \left(\rho_b \beta_b \right) \right]$. For the opposite direction of propagation, the numerators and the denominators in these fractions exchange places.

Numerical Examples. We consider a shear beam supported by elastic soil, as shown in Fig. 9. The densities of the soil and of the beam are assumed to be the same: $\rho_b = \rho_s = \rho =$ 2000 kg/m^3. The velocity of the shear waves in the soil is taken as $\beta_s = 250 m/s$, and in the building as $\beta_b = 100\, m/s$.

To describe nonlinear response and the development of permanent deformations in the beam, we introduce two dimensionless parameters: (1) dimensionless amplitude $\alpha = A / \left(H_b \varepsilon_b \right)$, where A is the amplitude of the pulse (Fig. 9), H_b is the height of the building, and ε_{yb} is the yielding strain in the building, and (2) dimensionless frequency $\eta = H_b / \left(\beta_b t_b \right)$, where $\beta_b t_d$ is one half of the wavelength of the wave in the building, β_b is the shear-wave velocity in the building, and t_d is the duration of the half-sine pulse.

To understand the development of the permanent strain in the nonlinear beam, we describe first the solution for the linear beam. The displacement and the strain for the linear beam are:

$$u(x,t) = A \sum_{j=1}^{\infty} k_j \left\{ \begin{array}{l} \sin \dfrac{\pi}{t_d} \left(t - t_{j-1} - \dfrac{x}{\beta_b} \right) \left[H\left(t - t_{j-1} - \dfrac{x}{\beta_b} \right) - H\left(t - t_{j-1} - \dfrac{x}{\beta_b} - t_d \right) \right] + \\ + \sin \dfrac{\pi}{t_d} \left(t - t_j + \dfrac{x}{\beta_b} \right) \left[H\left(t - t_j + \dfrac{x}{\beta_b} \right) - H\left(t - t_j + \dfrac{x}{\beta_b} - t_d \right) \right] \end{array} \right\} \quad (8)$$

and

$$\varepsilon(x,t) = A\frac{\pi}{\beta_b t_d}\sum_{j=1}^{\infty} k_j \left\{ \begin{array}{l} -\cos\dfrac{\pi}{t_d}\left(t - t_{j-1} - \dfrac{x}{\beta_b}\right)\left[H\left(t - t_{j-1} - \dfrac{x}{\beta_b}\right) - H\left(t - t_{j-1} - \dfrac{x}{\beta_b} - t_d\right)\right] \\ +\cos\dfrac{\pi}{t_d}\left(t - t_j + \dfrac{x}{\beta_b}\right)\left[H\left(t - t_j + \dfrac{x}{\beta_b}\right) - H\left(t - t_j + \dfrac{x}{\beta_b} - t_d\right)\right] \end{array} \right\} \quad (9)$$

where j is the order number of the passage of the wave on the path bottom-top-bottom in the building, $t_j = 2jH_b/\beta_b$ (j = 0,1,2,3,….,) is the time required for the wave to pass j times over the path bottom-top-bottom (two heights), $k_j = k_t k_r^{j-1}$ is the amplitude factor of the pulse in the soil in its j-th passage along the path bottom-top-bottom through the building, and k_t and k_r are coefficients defined by $k_{trB\to A}$ and $k_{refB\to B}$ above.

The odd terms in Eq. (8) and Eq. (9) describe the response to the pulse coming from below, while the even terms describe the response to the pulse arriving from above. For the shear-wave velocities in our example, $k_t = 10/7$ and $k_r = -3/7$. In Eq. (8) the displacement is positive for odd passages and negative for even passages. The displacement and velocity change sign after reflection from the soil-building interface and do not change sign after reflection from the top of the building. The strain changes sign after reflection from the top of the building and does not change sign after reflection from the building-soil interface. The constant that multiplies the series in Eq. (8) in terms of dimensionless amplitude and dimensionless frequency is $A\pi/(\beta_b t_d) = A_\varepsilon = \pi\alpha\eta\varepsilon_{yb}$.

To describe the occurrence of permanent strain, we consider two characteristic points in the building: (1) Point B $(x = 0)$ at the soil-building interface (point 3 in the grid, see Fig. 9), and (2) point T $(x = H_b - \beta_b t_b/2)$, where the amplitudes of the strain with the same sign meet after reflection from the top of the building. The location of this point is dependent upon the duration (wavelength) of the pulse. The first term in Eq. (8) is one if the argument of the cosine function is equal to t_d $(t - t_0 - x/\beta_b = t_d)$, and the second term is one if the argument of the second cosine function is equal to 0 $(t - t_1 + x/\beta_b = 0)$. The position of point T, where the strain amplitude is two times larger than the strain entering the beam, is at $x = H_b - \beta_b t_d/2$, and the time when this occurs is $t = H_b/\beta_b + t_d/2$. From Eq. (9) in the first passage of the pulse, $t < 2H_b/\beta_b$, and only the first term in the series exists. The strain at point B reaches its absolute maximum at the very beginning, during the entrance of the pulse into the building, and its value is $\left|\varepsilon^1_{B\max}\right| = \pi\alpha\eta\varepsilon_{yb}k_t$. If this strain is greater than the yielding strain in the building, ε_{yb}, a

permanent strain at the interface will develop, and the condition for occurrence of permanent strain at this point is $\left|\varepsilon^1_{B\max}\right| > \varepsilon_{yb}$, or, in terms of the dimensionless parameters,

$$\alpha\eta > (\pi k_t)^{-1} = (\beta_b + \beta_s)/(2\pi\beta_s) = C_B \ . \qquad (10B)$$

At point T (this point does not exist if $t_d > 2H_b/\beta_b$, and it coincides with point B if $t_d = 2H_b\beta_b$), from Eq. (9), the maximum strain during the first passage occurs at $t = H_b/\beta_b + t_d/2$, and its amplitude is $2A_\varepsilon \cdot k_t$. The condition for occurrence of the permanent strain is

$$\alpha\eta > (2\pi k_t)^{-1} = (\beta_b + \beta_s)/(4\pi\beta_s) = C_B/2 = C_T \ . \qquad (10T)$$

For the shear-wave velocities in our example $C_B = 0.2228$ and $C_T = 0.1114$.

For the above simple model, the occurrence, development, and amplitudes of permanent strains and displacements have been studied by Gicev and Trifunac (2006a,b). They found that for large ground-displacement pulses (large α) the maximum permanent strains occur mainly at the interface of the building with the soil, while for smaller amplitudes of pulses permanent strains occur closer to the top of the building. They distinguished three zones of the permanently deformed beam: (1) a permanently deformed zone at the bottom; (2) an intermediate zone, which is not deformed at its bottom part and is deformed in the top part; and (3) a non-deformed zone at the top of the beam. The occurrence and development of these zones depends upon the dimensionless excitation amplitudes and the dimensionless frequencies, and in particular on the conditions that lead to the occurrence of the first permanent strain (see Eqs. (10B) and (10T)). For large and long strong-motion pulses ($\eta \le 0.5$; first, the condition in Eq. (10B) is relevant), only zones 1 and 3 are present in the beam. For large amplitudes and short strong-motion pulses, all three zones develop and are present. For smaller excitation amplitudes (when the condition in Eq. (10B) cannot be satisfied for long pulses, and when the condition in Eq. (10T) is satisfied), only zones 2 and 3 exist in the beam. For larger values of η (when the condition in Eq. (10B) is satisfied) all three zones exist.

Gicev and Trifunac (2006a,b) found a similar situation for the occurrence of the maximum strains. For large and long pulses, maximum strain is located at the bottom of the building, and, as the pulses become shorter, peak strains occur at higher positions in the building. For some high frequencies of excitation, the maximum strain again appears at the bottom of the building because the loss of energy due to the development of the permanent strain at the bottom overcomes the effects of the wave reflections from the top of the building (Fig. 10).

Creation of large permanent deformation zones in the building by the incident waves absorbs some or most of the incident wave energy and can reduce or eliminate further wave propagation and the associated energy transport (Figs. 11 and 12). To the extent that the locations of the plastic deformation zones can be controlled by the design process, absorption of the incident-wave energy by structural members may become a new and powerful tool for performance-based design. To take advantage of such possibilities, the governing differential equations must be solved by the wave-propagation method.

Examples illustrated here show that for excitation of structures by large, near-field displacement pulses failure can occur anywhere in the building before the incident wave has completed its first travel from the foundation to the top of the building and back to the foundation ($2H_b / \beta_b$). Because this travel time is shorter (by ½) than the natural period of the structure on the fixed base, it is seen that the common response spectrum method of analysis (based on the vibrational formulation of the solution) cannot provide the required details for the design of structures for such excitation. The complexity of the outcome increases with amplitudes of excitation and depends upon the pulse duration. Because actual strong ground motion in the near field has at least several strong pulses, it can be seen that the complexity in real structures responding to strong earthquake motions will be even greater. In engineering approximation based on the vibrational solution of the problem and on the SDOF models, where the location of ductile response is predetermined by the simple modeling assumptions, this complexity cannot be included because of the modeling constraints. The outcome is that it is virtually impossible for simplified models to identify or to predict the location of damage. In contrast, for properly chosen wave propagation models, prediction and identification of damage is a natural and logical outcome of interaction between excitation and model properties. A good example of this can be found in Gicev and Trifunac (2007), who showed how a simple wave-propagation model can predict the actually observed location of damage.

V. Observations of Nonlinear Response

Invaluable for understanding and proper treatment of the actual nonlinear response, and for validation of vibration monitoring and analysis methods for real-life problems, are earthquake response data from well-instrumented, full-scale structures that have been damaged by an earthquake. Such data are rare and are not always freely available. An example of an instrumented building that has been damaged by an earthquake, and for which information about the damage and strong-motion data on the causative earthquake are available, is the former Imperial County Services Building in El Centro, California, which was severely damaged by the magnitude 6.6 Imperial Valley earthquake of October 15, 1979, and later demolished (Kojić et al. 1984; Todorovska and Trifunac 2007). Its transverse (NS) response was recorded by three vertical arrays (recording channels 1, 3, 7, 9, 10, and 11; see Fig. 13), and its longitudinal (EW) response was recorded by one vertical array (recording channels 4, 5, 6, and 13, also shown in Fig. 13).

For a simplified soil-structure interaction model of a building supported by a rigid foundation, the difference between the roof and base horizontal displacements during earthquake shaking is the sum of the horizontal displacements due to (1) horizontal deformation of the soil, (2) rigid-body rocking of the foundation, and (3) deformation of the structure. The estimated frequency from such data is referred to as system or "apparent" frequency, which differs from the fixed-base frequency of the building. While the fixed-base frequency depends only upon the properties of the structure, the apparent frequency depends also upon the stiffness of the foundation soil. The following relationship holds:

$$\frac{1}{\omega_{sys}^2} = \frac{1}{\omega_1^2} + \frac{1}{\omega_H^2} + \frac{1}{\omega_R^2}, \qquad (11)$$

where $\omega_{sys} = 2\pi\nu_{sys}$ is the soil-structure system frequency, ω_1 is the fundamental fixed-base frequency of the structure, and ω_H and ω_R are the horizontal and rocking frequencies, respectively, of a rigid structure on flexible soil (Luco et al. 1986).

Figure 14c shows that during earthquake shaking (Fig. 14a) the NS frequency of relative system response (Fig. 14b) dropped from $\nu \approx 2.12$ Hz in the early stage of response (at $t \approx 2$ s) to $\nu \approx 1.52$ Hz at $t \approx 6.8$ s ($\Delta\nu \approx 0.6$ Hz, $\Delta\nu/\nu \approx 28\%$), that it was constant during the interval $t \approx 6.8$–8.5 s, and that it dropped further to $\nu \approx 0.85$ Hz at $t \approx 12$ s ($\Delta\nu \approx 0.67$ Hz, $\Delta\nu/\nu \approx 44\%$). Then, toward the end of the recorded shaking, the frequency increased to $\nu \approx 1.15$ Hz ($\Delta\nu \approx 0.3$ Hz; $\Delta\nu/\nu \approx 35\%$). Early in the response ($t < 7$ s), the amplitudes of the first story drifts in the building were relatively small (< 0.5%), and the observed decrease of system frequency is believed to be due to changes in the soil and bonding between the soil and foundation. This was followed by a further decrease in the system frequency of about 44% (between 8 and 12 s). The first-story drifts in the building were large when this occurred (> 0.5% for NS), and the principal cause for this change is believed to be the damage, with the most severe damage occurring between 8 and 12 s after trigger. Near the end of the shaking, a 35% increase in system frequency was observed, suggesting system hardening, which is believed to be due to changes in the soil (Todorovska and Trifunac 2007).

Changes similar to what is shown in Fig. 14c were first observed following the San Fernando earthquake in California in 1971 (Udwadia and Trifunac 1974) and then during many subsequent earthquakes. It is known at present that many different factors can contribute to fluctuations of the system frequency, including rainfall, temperature fluctuations, changes in occupancy, remodeling and strengthening of buildings, wind, and earthquakes (Todorovska and Al Rjoub 2006). The simultaneous action of some of these factors and the associated time-dependent changes in the physical model contribute to complex and evolving system changes that make predictions of the dynamic response difficult.

VI. Future Directions

Well-designed structures are expected to have ductile behavior during the largest credible shaking, and a large energy reserve to at least delay failure if it cannot be avoided. As the structure finally enters large nonlinear levels of response, it absorbs the excess of the input energy through ductile deformation of its components. Thus, it is logical to formulate future earthquake-resistant design procedures in terms of the energy driving this process. From the mechanics point of view, this introduces nothing new, because the energy equations can be derived directly from the dynamic equilibrium equations. The advantage of using energy is that the duration of strong motion, the number of cycles to failure, and dynamic instability all can be addressed directly and explicitly. This, of course, requires scaling of the earthquake source and of the attenuation of strong motion described in terms of its wave energy. Trifunac et al. (2001d) reviewed the seismological aspects of empirical scaling of seismic wave energy, E_s, and showed how the radiated energy can be represented by the functionals of strong ground motion (Trifunac, 1989; 1993; 1994). They described the energy propagation and attenuation with distance and illustrated it for the three-dimensional geological structure of the Los Angeles basin during the 1994 Northridge, CA earthquake, then they described the seismic energy flow through the response of soil-foundation-structure systems, analyzed the energy available to excite the structure, and finally examined the relative response of the structure.

VI.1. Power Design

Figure 15 illustrates the cumulative wave energies recorded at a building site during two hypothetical earthquakes, E1 an E2, and presents a conceptual framework that can be used for development of the power design method. E1 results in a larger total shaking energy at the site and has a long duration of shaking, leading to relatively small average power, P1. E2 leads to smaller total shaking energy at the site but has short duration and thus greater power, P2. The power capacity of a structure cannot be described by one unique cumulative curve, as this depends upon the time history of shaking. For the purposes of this illustration, the line labeled "capacity envelope of the structure" can be thought of as an envelope of all possible cumulative energy paths for the response of this structure. Figure 15 implies that E1 will not damage this structure, but E2 will. Hence*, for a given structure, it is not the total energy of an earthquake event (and the equivalent energy-compatible relative velocity spectrum) but the rate with which this energy arrives and shakes the structure that is essential for the design of the required power capacity of the structure to withstand this shaking and to control the level of damage.*

Trifunac (2005) outlined the elementary aspects of such design based on the power of the incident wave pulses. He showed how this power can be compared with the capacity of the structure to absorb the incident wave energy and described the advantages of using the computed power of incident strong motion for design. Power (amplitude and duration) of the strong near-field pulses will determine whether the wave entering the structure will continue to propagate through the structure as a linear wave or will begin to create nonlinear zones (at first near the top and/or near the base of the structure; Gicev and Trifunac

2006a,b; 2007). For high-frequency pulses, the nonlinear zone, with permanent strains, can be created before the wave motion reaches the top of the structure—that is, before the interference of waves has even started to occur and lead to formation of mode shapes. Overall duration of strong motion (Trifunac and Novikova 1994) will determine the number of times the structure may be able to complete full cycles of response and the associated number of "minor" excursions into the nonlinear response range when the response is weakly non-linear (Gupta and Trifunac 1996), while the presence of powerful pulses of strong motion will determine the extent to which the one-directional quarter period responses (Trifunac 2005) may lead to excessive ductility demand, leading to dynamic instability and failure, precipitated by the gravity loads (Husid 1967). All of these possibilities can be examined and quantified deterministically by computation of the associated power capacities and power demands for different scenarios, for given recorded or synthesized strong-motion accelerograms, or probabilistically by using the methods developed for Uniform Hazard Analysis (Todorovska et al. 1995).

VII. Bibliography

Books and Reviews

Beltrami, E. (1987). *Mathematics for Dynamic Modeling*, J. Wiley and Sons, New York.

Kapitaniak, T. (1991). *Chaotic Oscillations in Mechanical Systems*, Manchester Univ. Press, Manchester, UK.

Kuhn, T. (1962). *The Structure of Scientific Revolutions,* The University of Chicago Press, Chicago.

Lichtenberg, A.J., and Lieberman, M.A. (1983). *Regular and Stochastic Motion,* Springer-Verlag, New York.

Rasband, S.N. (1990). *Chaotic Dynamics of Nonlinear Systems*, J. Wiley and Sons, New York.

Primary Literature

Biot, M.A. (1932). Vibrations of buildings during earthquakes, Chapter II in Ph.D. Thesis No. 259, entitled "Transient Oscillations in Elastic System," Aeronautics Department, Calif. Inst. of Tech., Pasadena.

Biot, M.A. (1933). Theory of elastic systems vibrating under transient impulse with an application to earthquake-proof buildings, *Proc. National Academy of Sciences*, 19(2), pp. 262–268.

Biot, M.A. (1934). Theory of vibration of buildings during earthquakes, *Zeitschrift für. Angewandte Matematik und Mechanik*, 14(4), pp. 213–223.

Biot, M.A. (2006). Influence of foundation on motion of blocks, *Soil Dynamics & Earthquake Engrg.*, 26(6–7), 486–490.

Bycroft, G.N. (1980). Soil-foundation interaction and differential ground motions, *Earthquake Engineering and Structural Dynamics*, 8(5), 397–404.

Fujino, Y., and Hakuno, M. (1978). Characteristics of elasto-plastic ground motion during an earthquake. *Bull. Earthquake Res. Institute*, Tokyo Univ., 53, 359–378.

Gicev, V. (2005). Investigation of soil-flexible foundation-structure interaction for incident plane SH waves, Ph.D. Dissertation, Dept. of Civil Engineering, Univ. Southern California, Los Angeles, CA.

Gicev, V., and Tifunac, M.D. (2006a). Rotations in the transient response of nonlinear shear beam, *Dept. of Civil Engineering Report* CE 06-02, Univ. Southern California, Los Angeles, CA.

Gicev, V., and Tifunac, M.D. (2006b). Non-linear earthquake waves in seven-story reinforced concrete hotel, *Dept. of Civil Engineering, Report* CE 06-03, Univ. Southern California, Los Angeles, CA.

Gicev, V., and Tifunac, M.D. (2007). Permanent deformations and strains in a shear building excited by a strong motion pulse, *Soil Dynamics and Earthquake Engineering*, **27**(8), 774-792.

Crutchfield, J.P. (1992). Knowledge and meaning, in Modeling Complex Phenomena, L. Lam and V. Naroditsky (Eds.), 66-101, Springer-Verlag, N.York.

Gupta, I.D., and Trifunac, M.D. (1996). Investigation of nonstationarity in stochastic seismic response of structures, *Dept. of Civil Eng. Report CE 96-01*, Univ. of Southern California, Los Angeles, Ca.

Gwinn, E.G., and Westervelt, R.M. (1985). Intermittent chaos and low-frequency noise in the driven damped pendulum, *Phy.Rev. Lett.*, 54(15), 1613–1616.

Hackett, K., and Holmes, P.J. (1985). Josephson Junction, annulus maps, Birkhoff Attractors, horsehoes and rotation sets, *Center for Applied Math. Report,* Cornell University.

Holmes, P.J. (1979). A nonlinear oscillator with a strange attractor, *Philos. Trans. R. Soc. London A*, 292, 419–448.

Holmes, P.J. (1982). The dynamics of repeated impacts with a sinusoidally vibrating table, *J. Sound Vib.,* 84,173–189.

Holmes, P.J. (1985). Dynamics of a nonlinear oscillator with feedback control, *J. of Dynamics Systems, Measurement and Control,* 107, 159–165.

Holmes, P.J., and Moon, F.C. (1983). Strange Attractors and Chaos in Nonlinear Mechanics, *J. Appl. Mech.,* 50, 1021–1032.

Husid, R. (1967). Gravity effects on the earthquake response of yielding structures, *Ph.D. Thesis*, Calif. Inst. of Tech., Pasadena.

Jalali, R., and Trifunac, M.D. (2007). Strength-reduction factors for structures subjected to differential near-source ground motion, *Indian Society of Earthquake Technology Journal* , 44(1), (in press).

Kojić, S., Trifunac, M.D., and Anderson, J.C. (1984). A post-earthquake response analysis of the Imperial County Services building in El Centro. *Report CE 84-02,* University of Southern California, Department of Civil Engineering, Los Angeles.

Lee, V.W. (1979). Investigation of three-dimensional soil-structure interaction, *Department of Civil Engineering,* Report CE. 79-11, Univ. of Southern California, Los Angeles.

Lee, V.W., and Trifunac, M.D. (1982). Body wave excitation of embedded hemisphere, *ASCE, EMD*, 108(3), 546–563.

Lee, V.W., and Trifunac, M.D. (1985). Torsional accelerograms, *Int. J. Soil Dynamics and Earthquake Engineering*, 4(3), 132–139.

Lee, V.W., and Trifunac, M.D. (1987). Rocking strong earthquake accelerations, *Int. J. Soil Dynamics and Earthquake Eng*., 6(2), 75–89.

Levin, P.W.,and Koch, B.P. (1981). Chaotic behavior of a parametrically excited damped pendulum, *Phys. Lett. A.* 86(2), 71–74.

Lighthill, J. (1994). Chaos: A historical perspective, in *Nonlinear Dynamics and Predictability of Geophysical Phenomena,* W.I. Newman, A. Gabrielov, and D. Turcotte (eds.), Geophysical Monograph 83, IUGG, Vol. 18, 1–5.

Lomnitz, C, and Castanos, H. (2006). Earthquake hazard in the valley of mexico: entropy, structure, complexity, Ch. 27 in *Earthquake Source Asymmetry, Structural Media and Rotation Effects*, R. Teisseyre, M. Takeo, and E. Majewski (eds.), Springer, Heidelberg, Germany.

Luco, J.E., Wong, H.L., and Trifunac, M.D. (1986). Soil-structure interaction effects on forced vibration tests. *Dept. of Civil Engrg., Rep. No. 86-05,* University of Southern California, Los Angeles.

McLaughlin, J.B. (1981). Period-doubling bifurcations and chaotic motion for a parametrically forced pendulum, *J. Stat. Phys.,* 24(2), 375–388.

Miles, J. (1984a). Resonant motion of spherical pendulum, *Physica*, 11D, 309–323.

Miles, J. (1984b). Resonantly forced motion of two quadratically coupled oscillators, *Physica,* 13D, 247–260.

Moon, F.C. (1980a). Experiments on chaotic motions of a forced nonlinear oscillator: Strange attractors, *ASME J. Appl. Mech.,* 47, 638–644.

Moon, F.C. (1980b). Experimantal models for strange attractor vibration in elastic systems, in *New Approaches to Nonlinear Problems in Dynamics,* P.J. Holmes (ed.), 487–495.Moon, F.C., and Holmes, P.J. (1979). A magnetoelastic strange attractor*, J. Sound Vib.,* 65(2), 275–296; A magneto-elastic strange attractor, *J. Sound Vib.,* 69(2), 339.

Moon, F.C., and Holmes, W.T. (1985). Double Poincare sections of a quasi-periodically forced, chaotic attractor, *Phys. Lett. A,* 111(4), 157–160.

Moon, F.C., and Shaw, S.W. (1983). Chaotic vibration of beams with nonlinear boundary conditions, *J. Nonlinear Mech.,* 18, 465–477.

Poddar, B., Moon, F.C., and Mukherjee, S. (1986). Chaotic motion of an elastic-plastic beam, *J. Appl. Mech., ASME,* 55(1), 185–189.

Reitherman, R. (2006). The effects of the 1906 earthquake in california on research and education, *Earthquake Spectra,* (22)S2, S207–S236.

Richter, P.H., and Scholtz, H.J. (1984). Chaos and classical mechanics: The double pendulum, in *Stochastic Phenomena and Chaotic Behavior in Complex Systems*, P. Schuster (ed.), Springer-Verlag, Berlin, 86–97.

Shaw, S.W. (1985). The dynamics of a harmonically excited system having rigid amplitude constraints, parts 1, 2, *J. Applied mechanics,* 52(2), 453–464.

Shaw, S., and Holmes, P.J. (1983). A periodically forced piecewise linear oscillator, *J. Sound Vib.,* 90(1), 129–155.

Sorrentino, L. (2007). The early entrance of dynamics in earthquake engineering: Arturo Danusso's contribution, *ISET Journal*, 44(1), (in press).

Todorovska, M.I., and Al Rjoub, Y. (2006). Effects of rainfall on soil-structure system frequency: Examples based on poroelasticity and comparison with full-scale measurements, *Soil Dynamics and Earthquake Engineering*, 26(6–7), 708–717.

Todorovska. M.I., & Trifunac, M.D. (1990). Note on excitation of long structures by ground waves. *ASCE, EMD*, 116(4), 952–964, and Errata in 116, 1671.

Todorovska, M.I., Gupta, I.D., Gupta, V.K., Lee, V.W., and Trifunac, M.D. (1995). *Selected topics in probabilistic seismic hazard analysis*, Dept. of Civil Eng. Report No. CE 95-08, Univ. of Southern California, Los Angeles.

Todorovska, M.I., and Trifunac, M.D. (2007). Earthquake Damage Detection in the Imperial County Services Building I: the Data and Time-Frequency Analysis, *Soil Dynamics and Earthquake Engineering,* **27**(6), 564-576.

Trifunac, M.D. (1989). Dependence of Fourier spectrum amplitudes of recorded strong earthquake accelerations on magnitude, local soil conditions and on depth of sediments, *Earthquake Eng. and Struct. Dynam*., 18(7), 999–1016.

Trifunac, M.D. (1993). Long-period Fourier amplitude spectra of strong motion acceleration, *Soil Dynam. and Earthquake Eng*., 12(6), 363–382.

Trifunac, M.D. (1994). Q and High-Frequency Strong-Motion Spectra, *Soil Dynam. and Earthquake Eng*., 13(3), 149–161.

Trifunac, M.D. (2003). *70th Anniversary of Biot Spectrum, 23rd Annual ISET Lecture,* Indian Society of Earthquake Technology, (40)1, 19–50.

Trifunac, M.D. (2005). Power design method*. Proc. of Earthquake Engineering in the 21st Century to Mark 40th Anniversary of IZIIS-Skopje,* August 28–September 1, Skopje and Ohrid, Macedonia.

Trifunac, M.D. (2006). Effects of torsional and rocking excitations on the response of structures, Ch. 39 in *Earthquake Source Asymmetry, Structural Media, and Rotation Effects*, R. Teisseyre, M. Takeo, and E. Majewski (eds.), Springer, Heidelberg, Germany.

Trifunac, M.D., and Gicev, V. (2006). Response Spectra for Differential Motion of Columns, Paper II: Out of-Plane Response, *Soil Dynamics and Earthquake Engineering*, 26(12), 1149–1160.

Trifunac, M.D., and Novikova, E.I., (1994). State-of-the-art review on strong motion duration, *10th European Conf. on Earthquake Eng*., I, 131–140.

Trifunac, M.D., and Todorovska, M.I. (1997). Response spectra and differential motion of columns, *Earthquake Eng. and Structural Dyn.*, 26(2), 251–268.

Trifunac, M.D., Ivanovic, S.S., and Todorovska, M.I. (2001a). Apparent periods of a building I: Fourier analysis, *J. of Struct. Engrg*, ASCE, 127(5), 517–526.

Trifunac, M.D., Ivanovic, S.S., and Todorovska, M.I. (2001b). Apparent periods of a building II: Time-frequency analysis, *J. of Struct. Engrg*, ASCE, 127(5), 527–537.

Trifunac, M.D., Hao, T.Y., and Todorovska, M.I. (2001c). Response of a 14-story reinforced concrete structure to nine earthquakes: 61 years of observation in the hollywood storage building, *Dept. of Civil Engrg., Report* CE 01-02, Univ. of Southern California, Los Angeles.

Trifunac, M.D., Hao, T.Y., and Todorovska, M.I. (2001d). On energy flow in earthquake response, Dept. of Civil Eng., *Report No. CE 01-03*, Univ. of Southern California, Los Angeles.

Udwadia, F.E., and M.D. Trifunac (1974). Time and amplitude dependent response of structures, *Earthquake Engrg Struct. Dynam*., 2, 359–378.

Ueda, Y. (1980). Steady motions exhibited by Duffing's equation: A picture book of regular and chaotic motions, *New Approaches to Nonlinear Problems in Dynamics*, P.J. Holmes (ed.) SIAM, Philadelphia.

Veletsos, A.S., and Newmark, N.M. (1960). Effect of inelastic behavior on the response of simple systems to earthquake motions, *Proc.2nd World Conf. On Earthquake Engineering,* Vol. II, 859-912.

Veletsos, A.S., and Newmark, N.M. (1964). *Response spectra for single-degree-of-freedom elastic and inelastic systems*, Rep. No. RTD-TDR-63-3096, Vol. III, Air Force Weapons Lab., Albuquerque, NM.

Wong, H.L., and Trifunac, M.D. (1979). Generation of artificial strong motion accelerograms, *Int. J. Earthquake Engineering Struct. Dynamics*, 7(6), 509–527.

FIGURE CAPTIONS

Fig. 1. Chaos diagram showing regions of chaotic, chaotic and periodic, periodic (I, II, III, etc), and sub-harmonic (4/3, 3/2, 5/3, etc.) motions for a nonlinear equation as functions of non-dimensionalized damping and forcing amplitude (from Ueda 1980).

Fig. 2. Single-degree-of-freedom system (SDOF) representation of a building (inverted pendulum) with equivalent mass m_b and mass-less column height h, experiencing rocking ψ_r due to horizontal motion of its base Δ_x.

Fig. 3. Single-degree-of-freedom system (SDOF) representation of a building (inverted pendulum), with equivalent mass m_b, moment of inertia (about O) I_b, and a mass-less column of height h, experiencing relative rocking ψ_r due to horizontal, vertical, and rocking motions of its foundation (Δ_x, Δ_z, and ϕ_y), which result from soil-structure interaction when excited by incident wave motion.

Fig. 4. Six components of motion (three translations and three rotations) $\{\Delta_x, \Delta_y, \Delta_z, \phi_x, \phi_y, \phi_z\}$ of point B, and six components of force (three forces and three moments) $\{F_{ext}\} = \{F_{bx}, F_{by}, F_{bz}, M_{bx}, M_{by}, M_{bz}\}$, that the structure exerts on the foundation at B.

Fig. 5. Schematic representation of the deformation of columns accompanying differential wave excitation of long structures for out-of-plane response (top) and in-plane response (bottom) when SH or Lave waves (top) or Rayleigh waves (bottom) propagate along the longitudinal axis of a structure.

Fig. 6. Bi-linear representation of stiffness (yielding at (u_y, f_y)), overturning moment of gravity force ($m_b g \sin\psi$), critical rocking angle $\psi_{r,cr}$, and meta-stable region ($0 < \psi_r < \psi_{r,cr}$) for an SDOF system.

Fig. 7. The structure deformed by the wave, propagating from left to right, with phase velocity C_x, for the case of $+v_{g_i}$ ("up" motion). Different column rotations ψ_1 and ψ_2 result from different translations and rotations at supports 1 and 2 (from Jalali and Trifunac 2007).

Fig. 8 Example of the effects of the differential ground motion on the strength-reduction factors R_y at the four corners of the structure in Fig. 7, subjected to horizontal, vertical, and rocking components of the fault-parallel displacement, for downward vertical motion ($-v_{g_i}$) for earthquake magnitude M = 8, ductility $\mu = 8$, and delay at the right support $\tau = 0.05$ s. The amplitudes of the piecewise straight representation of the classical R_y are shown for comparison (Jalali and Trifunac 2007). $(R_y)_{\min}$ shows the smallest values of the R-factors, which for the set of conditions in this example are determined by the response at the top left corner (for periods shorter than 0.1 s), at the bottom right corner (for periods between 0.1 and 0.35 s), and at the top right corner (for periods longer than 0.35 s).

Fig. 9. Shear beam (building) (left) and incoming strong-motion displacement pulse (right) in the soil.

Fig. 10. Permanent displacements ($u_{\max} = 0.126m$) (top), and permanent strains ($\varepsilon_1 = 0.31, \varepsilon_2 = 0.32, \varepsilon_3 = 0.20$) (bottom), along the building versus dimensionless frequency η and for dimensionless amplitude $\alpha = 0.3$.

Fig. 11. Linear displacements along the normalized length of the beam, $\chi = x / H_b$, versus normalized time $\tau = \beta_b t / 2H_b$, for dimensionless pulse amplitude $\alpha = 0.03$ and dimensionless frequency $\eta = 3$.

Fig. 12. Nonlinear displacements along the normalized length of the beam, $\chi = x / H_b$, versus normalized time $\tau = \beta_b t / 2H_b$ for dimensionless pulse amplitude $\alpha = 0.3$ and dimensionless frequencies $\eta = 3$ (top) and $\eta = 0.41$ (bottom).

Fig. 13. Layout of the seismic monitoring array in the ICS building (dots, without arrows, show the NS recording channels).

Fig. 14. Time-frequency analysis for the NS response of the ICS building: (a) ground acceleration, (b) relative roof response, and (c) system frequency versus time.

Fig. 15. Schematic comparison of strong-motion power demands E1 and E2 with an envelope of structural power capacity.

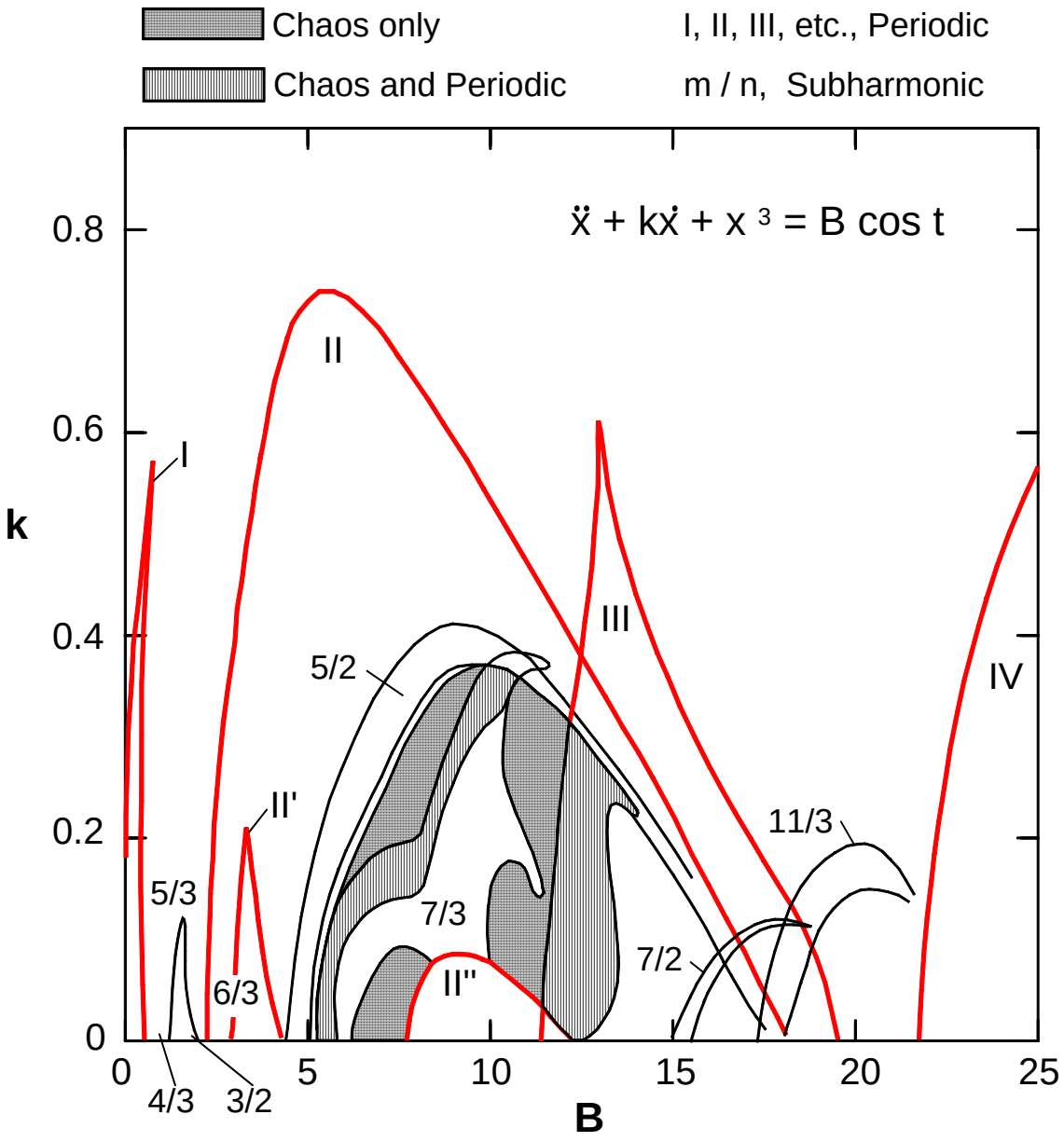
Chaos only
Chaos and Periodic
I, II, III, etc., Periodic
m / n, Subharmonic
ẍ + kẋ + x ³ = B cos t
k
B
0.8
0.6
0.4
0.2
0
0
5
10
15
20
25
I
II
II'
II"
III
IV
5/2
5/3
6/3
7/3
7/2
11/3
4/3
3/2

Fig. 1

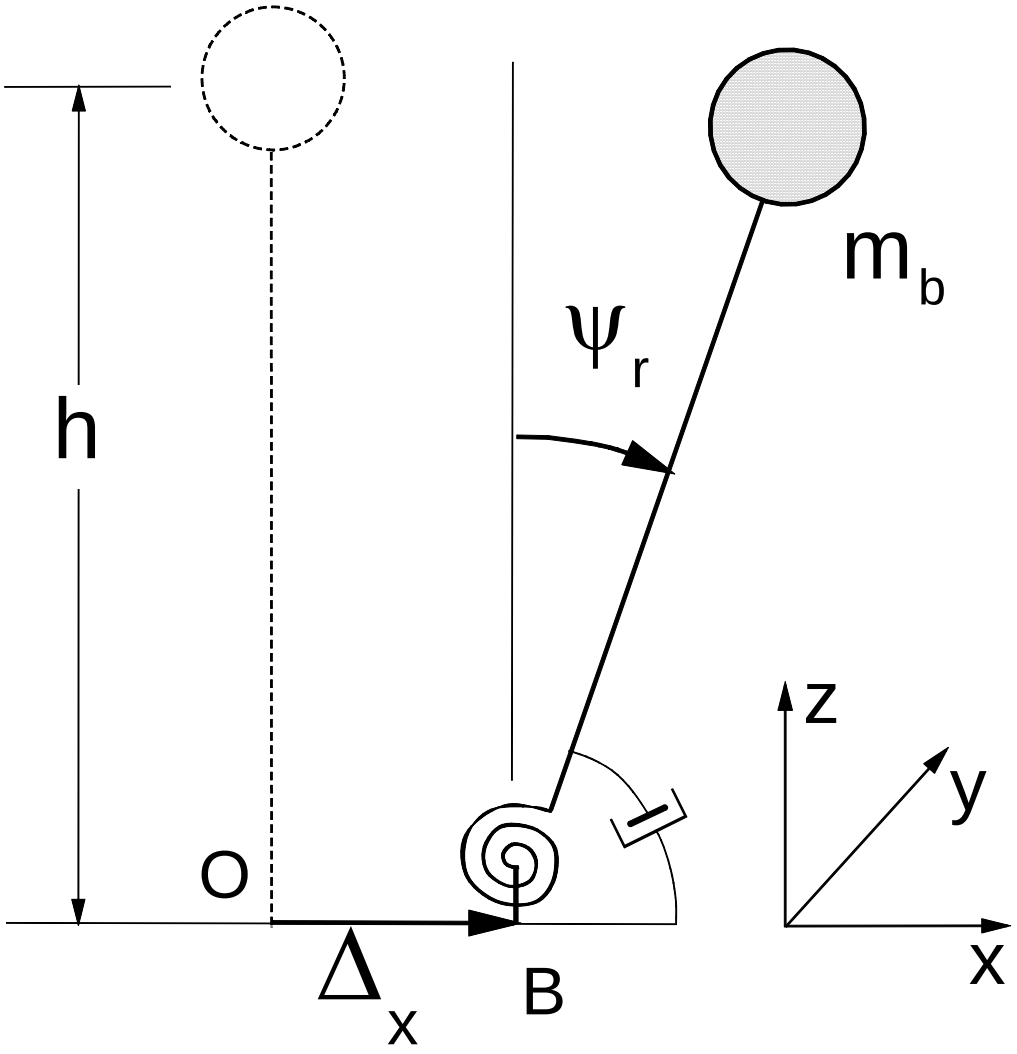

Fig.2

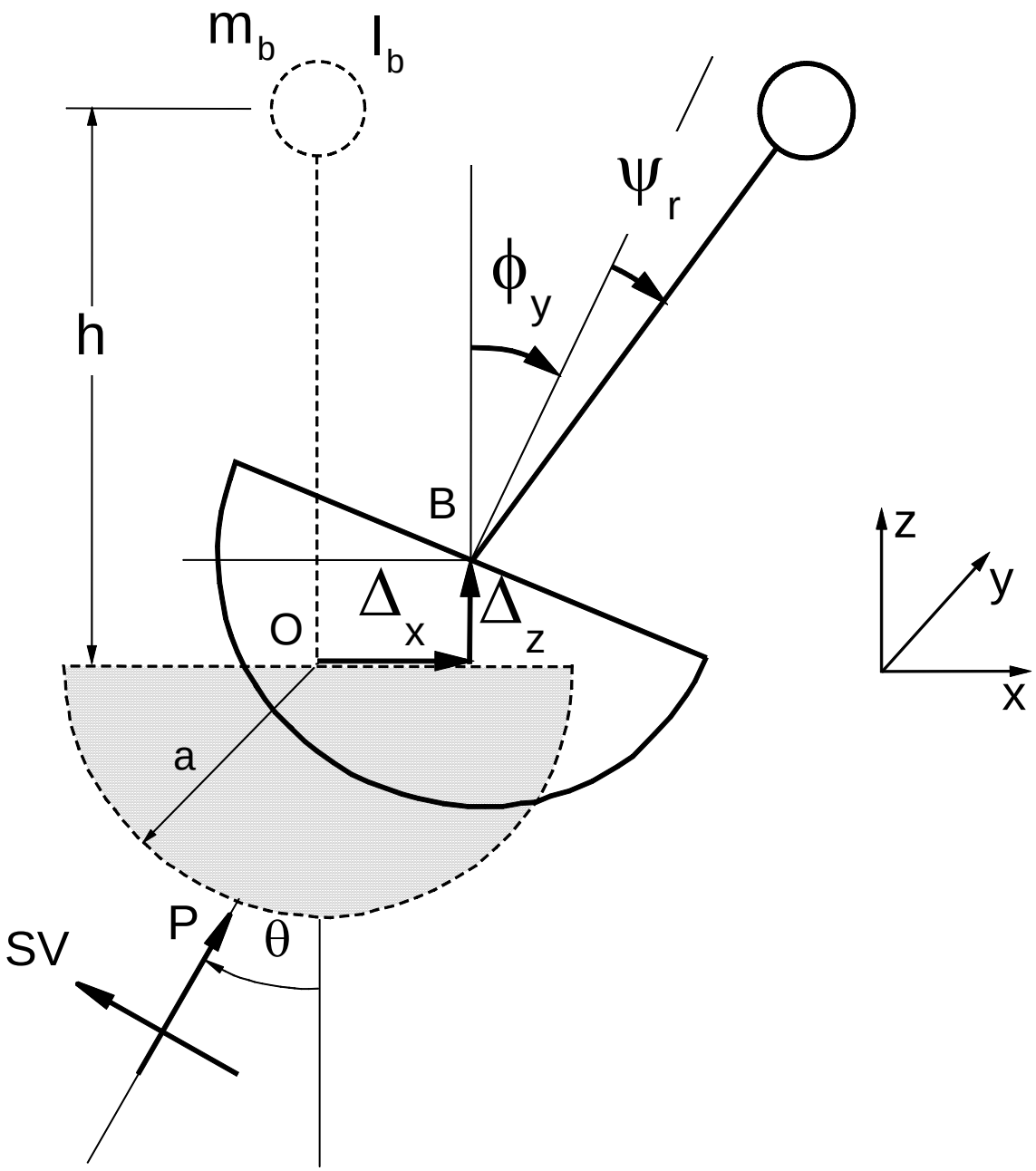

Fig. 3

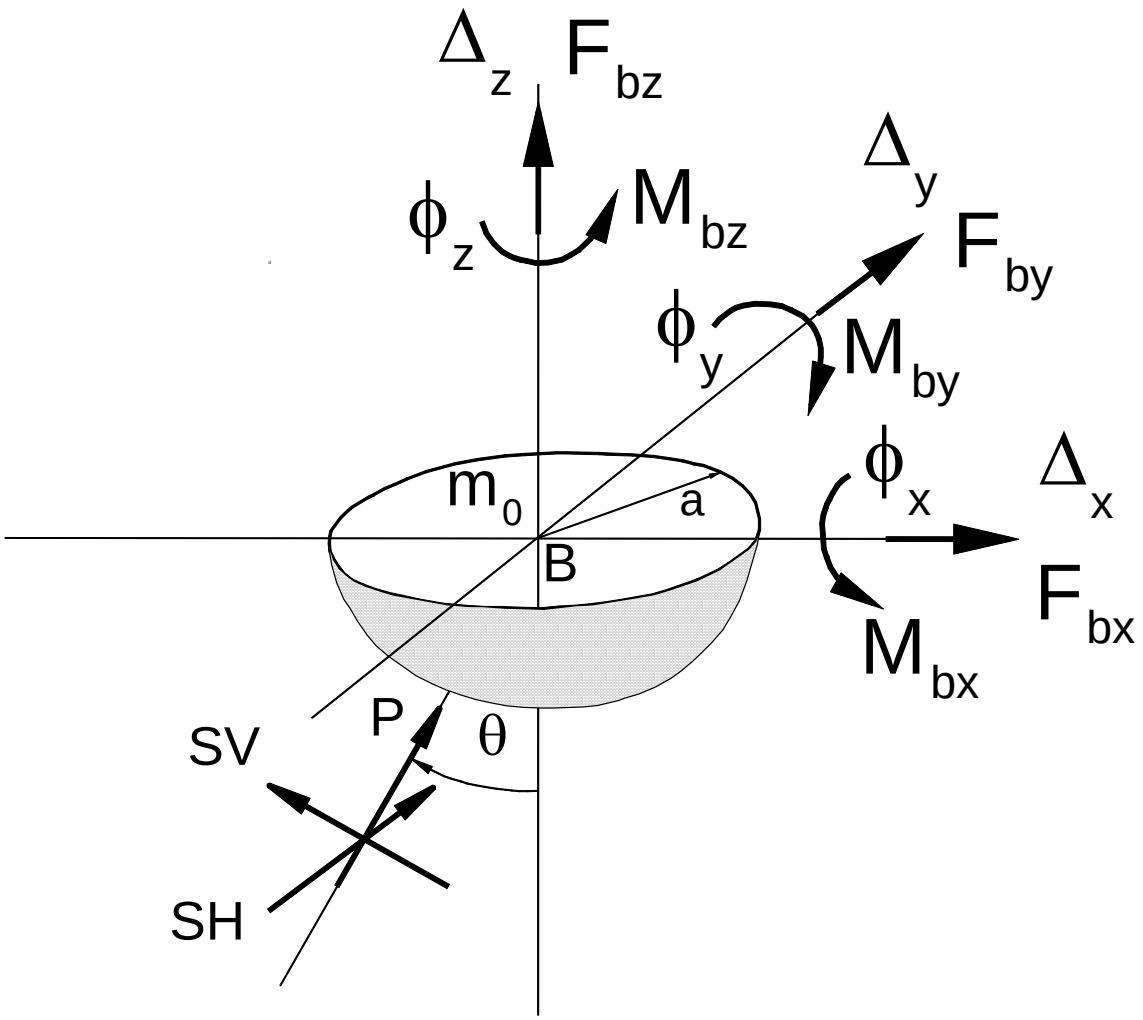

Fig. 4

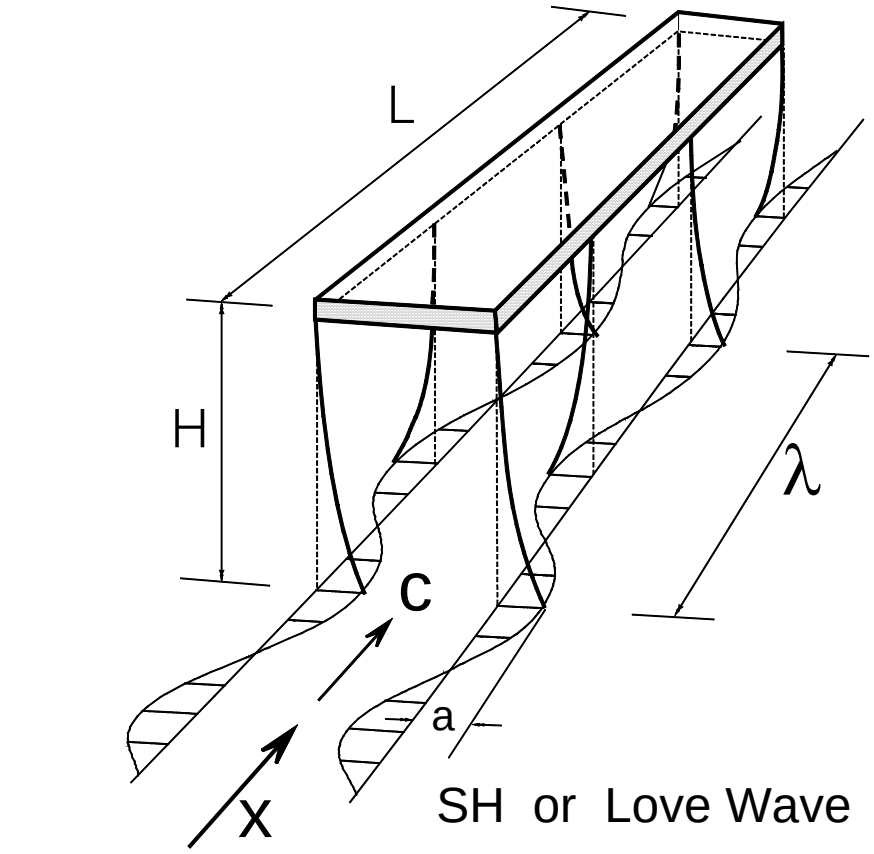

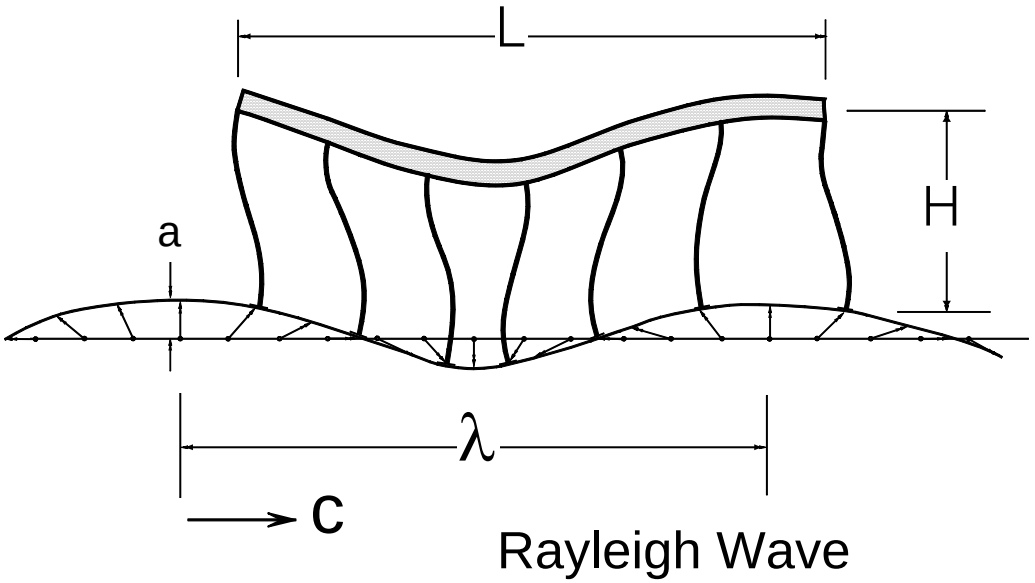

Fig. 5

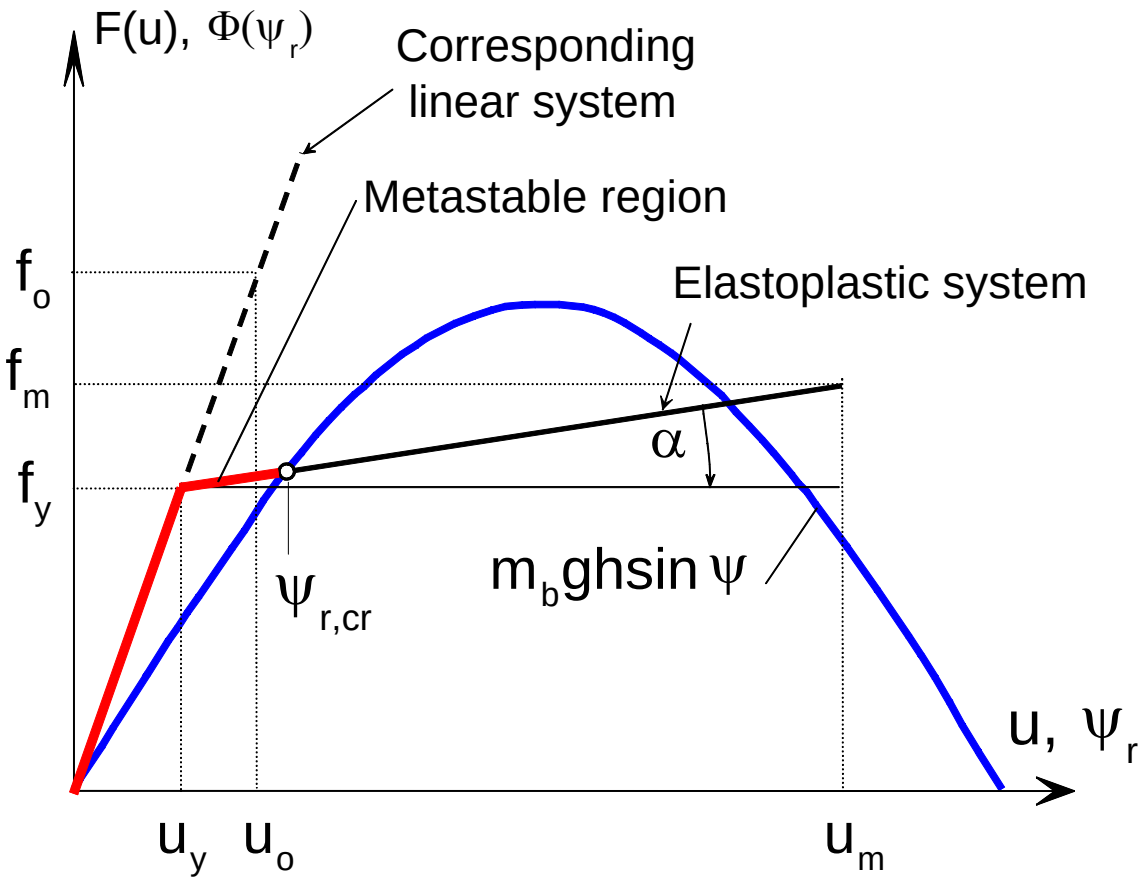
F(u), Φ(ψ_r)
Corresponding
linear system
Metastable region
Elastoplastic system
f_o
f_m
f_y
α
m_b ghsin ψ
ψ_r,cr
u, ψ_r
u_y
u_o
u_m

Fig.6

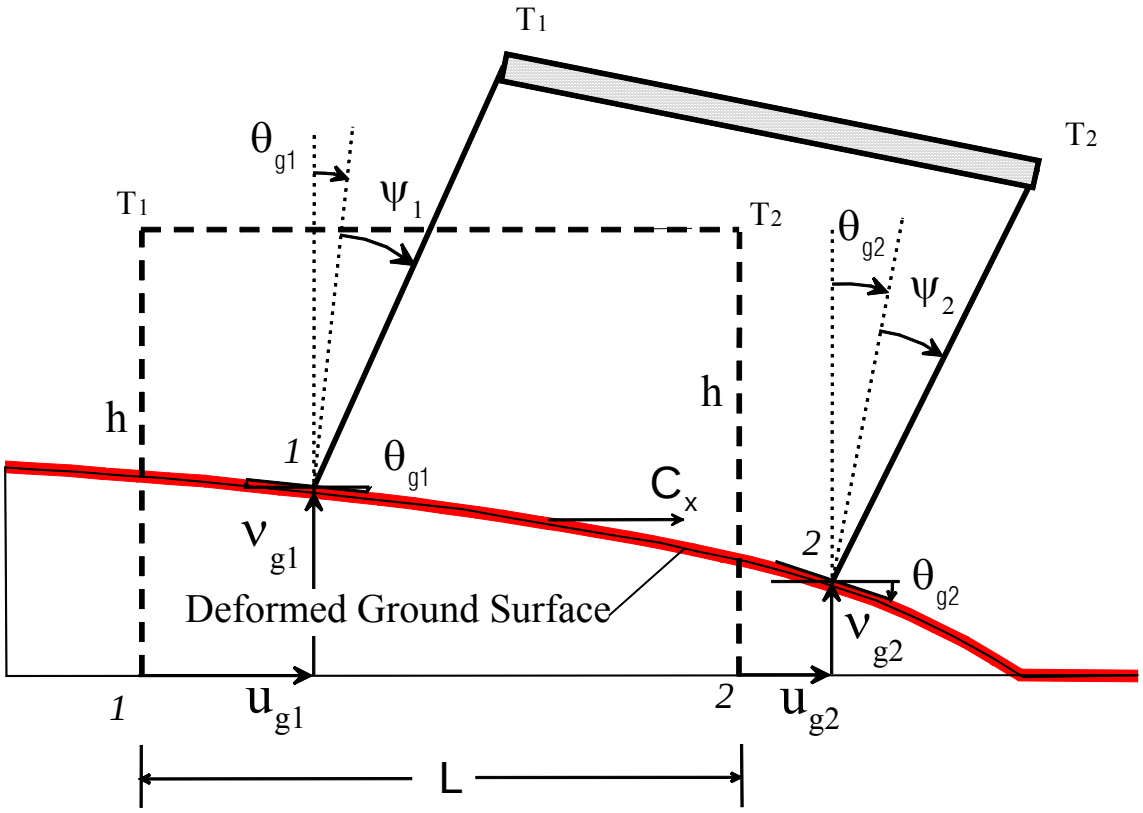
T1
T2
θg1
ψ1
T1
T2
θg2
ψ2
h
h
1
θg1
Cx
νg1
2
θg2
Deformed Ground Surface
νg2
1
ug1
2
ug2
L

Fig. 7

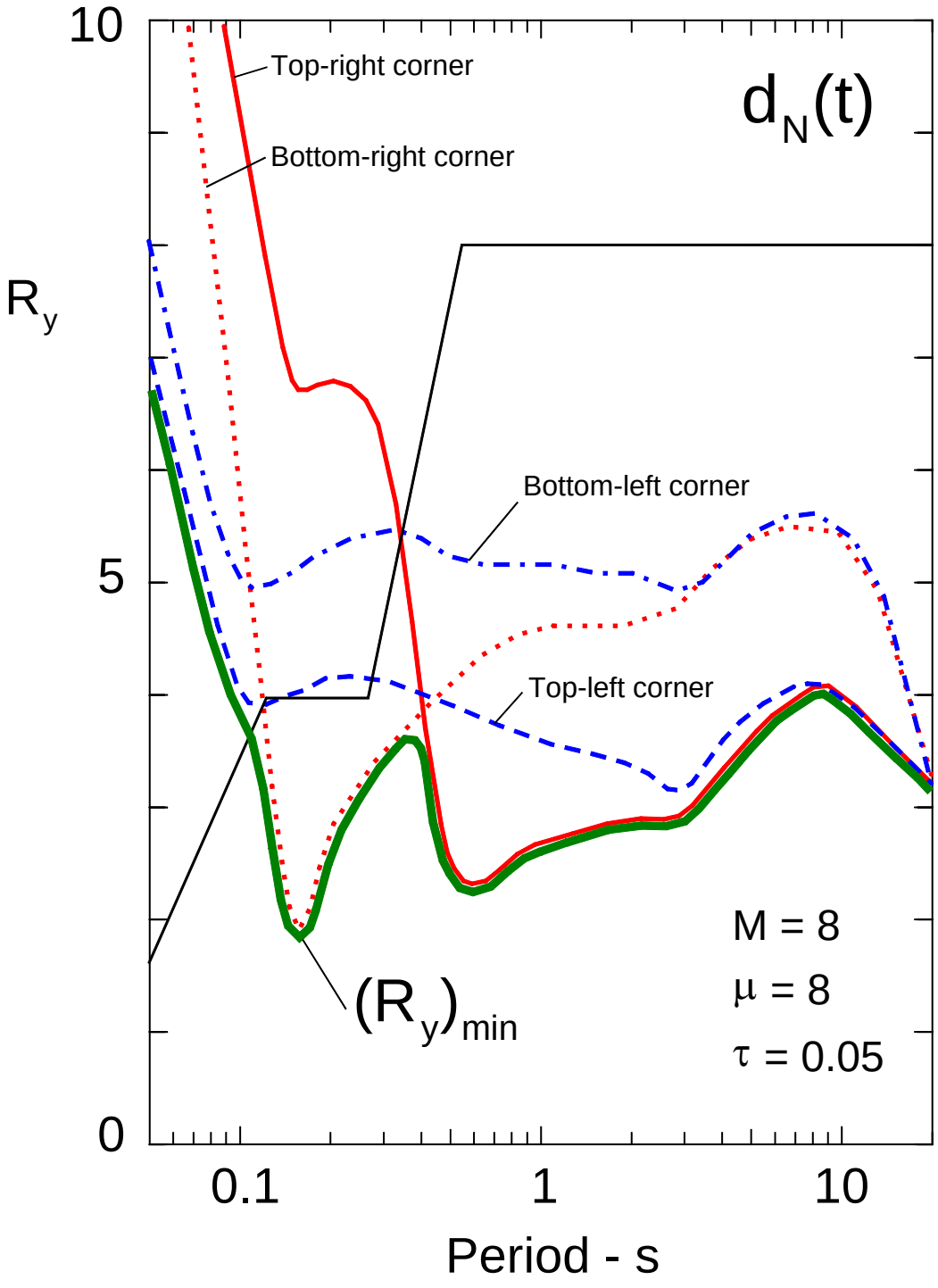
10
5
0
R_y
Top-right corner
Bottom-right corner
$d_N(t)$
Bottom-left corner
Top-left corner
$(R_y)_{min}$
M = 8
μ = 8
τ = 0.05
0.1
1
10
Period - s

Fig. 8

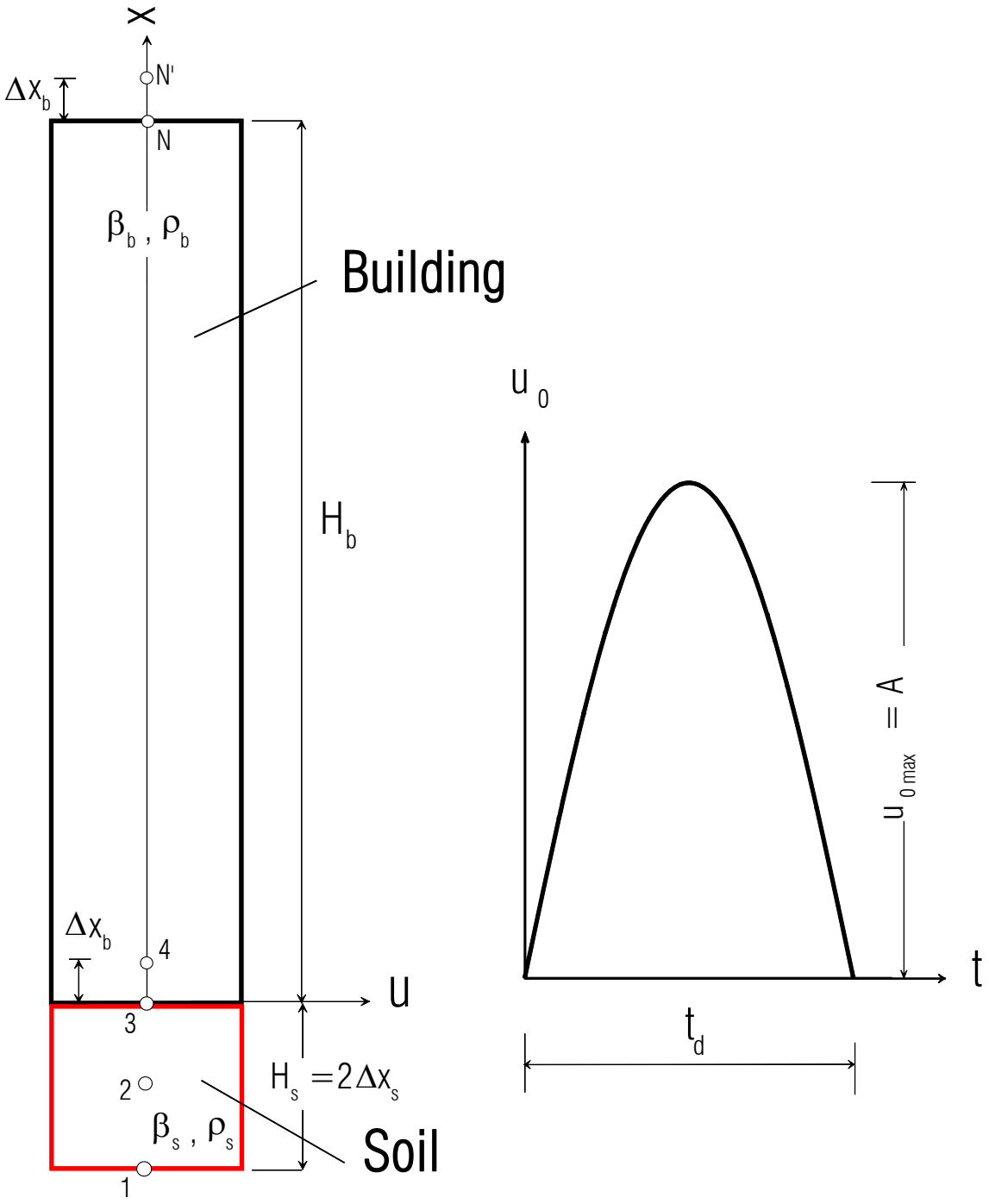
x
N'
N
Δx_b
β_b , ρ_b
Building
H_b
Δx_b
4
3
u
2
$H_s = 2\Delta x_s$
β_s , ρ_s
Soil
1
u_0
$= A$
$u_{0\,max}$
t
t_d

Fig. 9

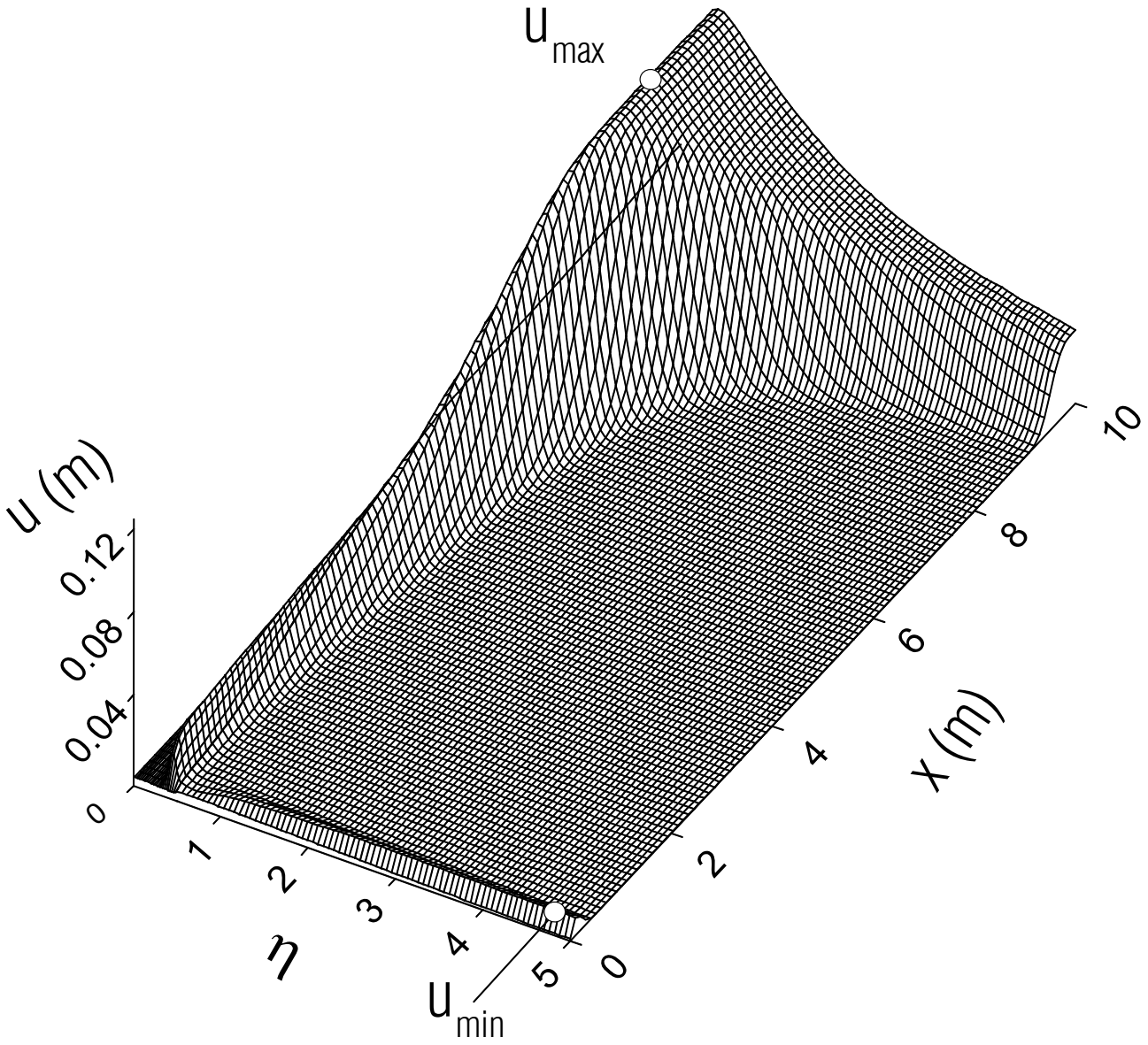

Fig. 10a

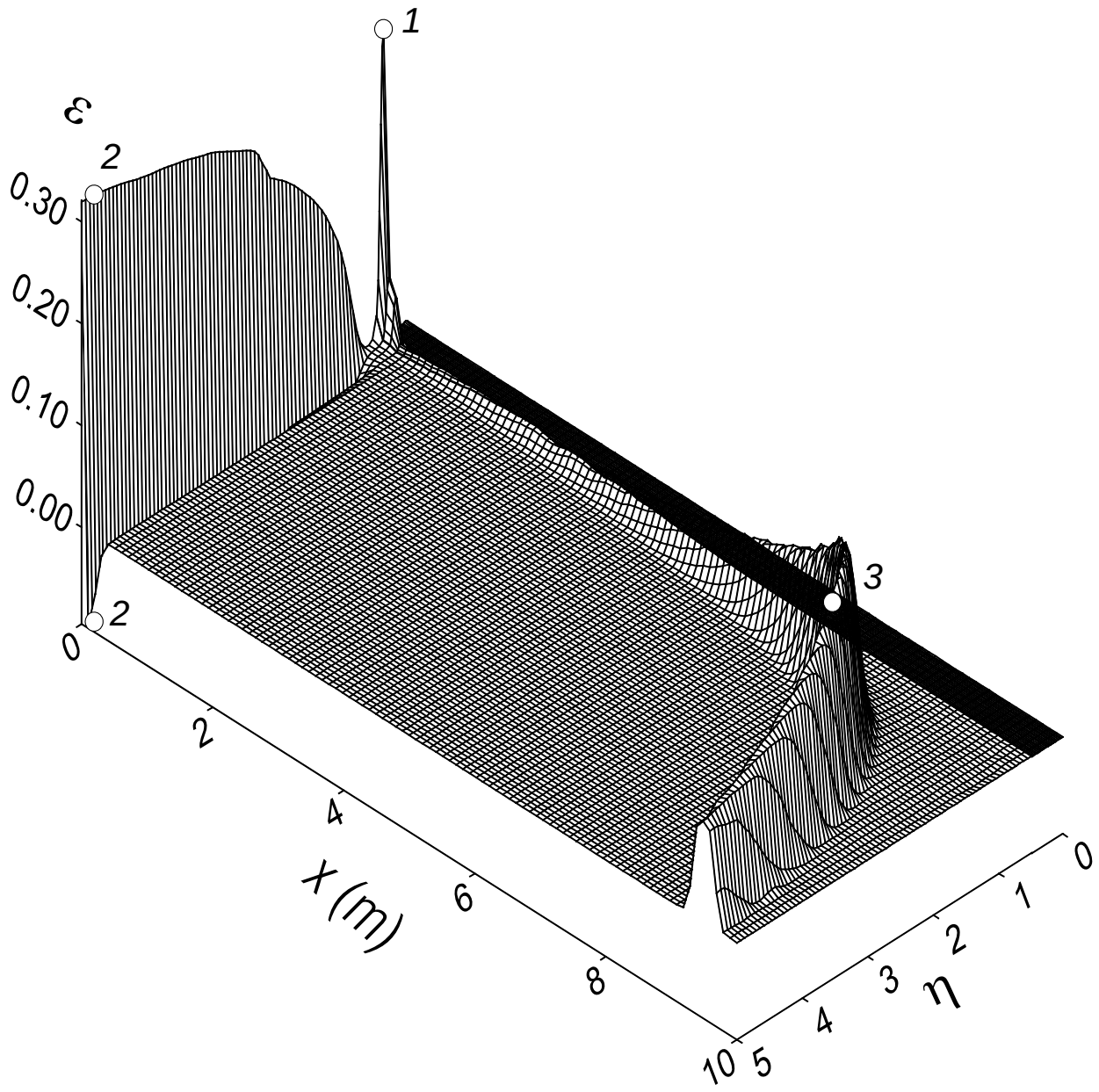

Fig. 10b

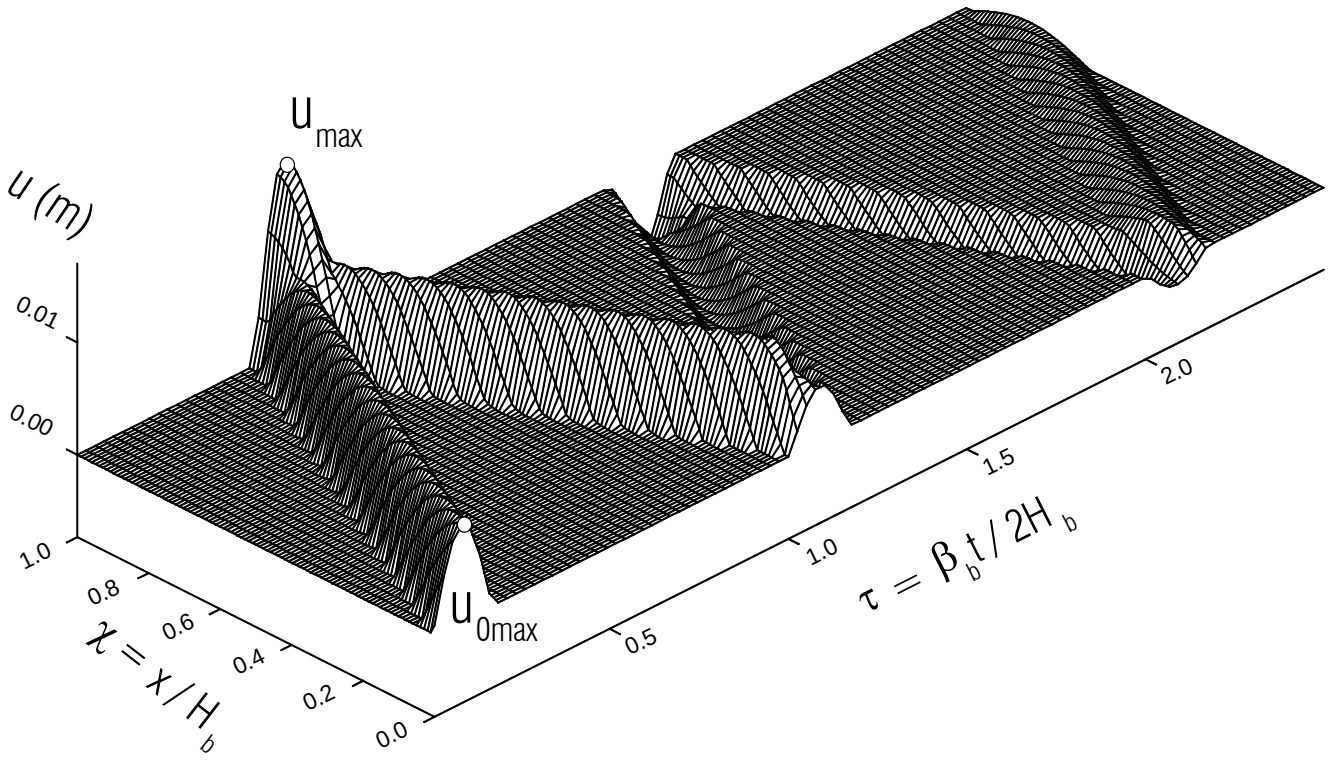

Fig. 11

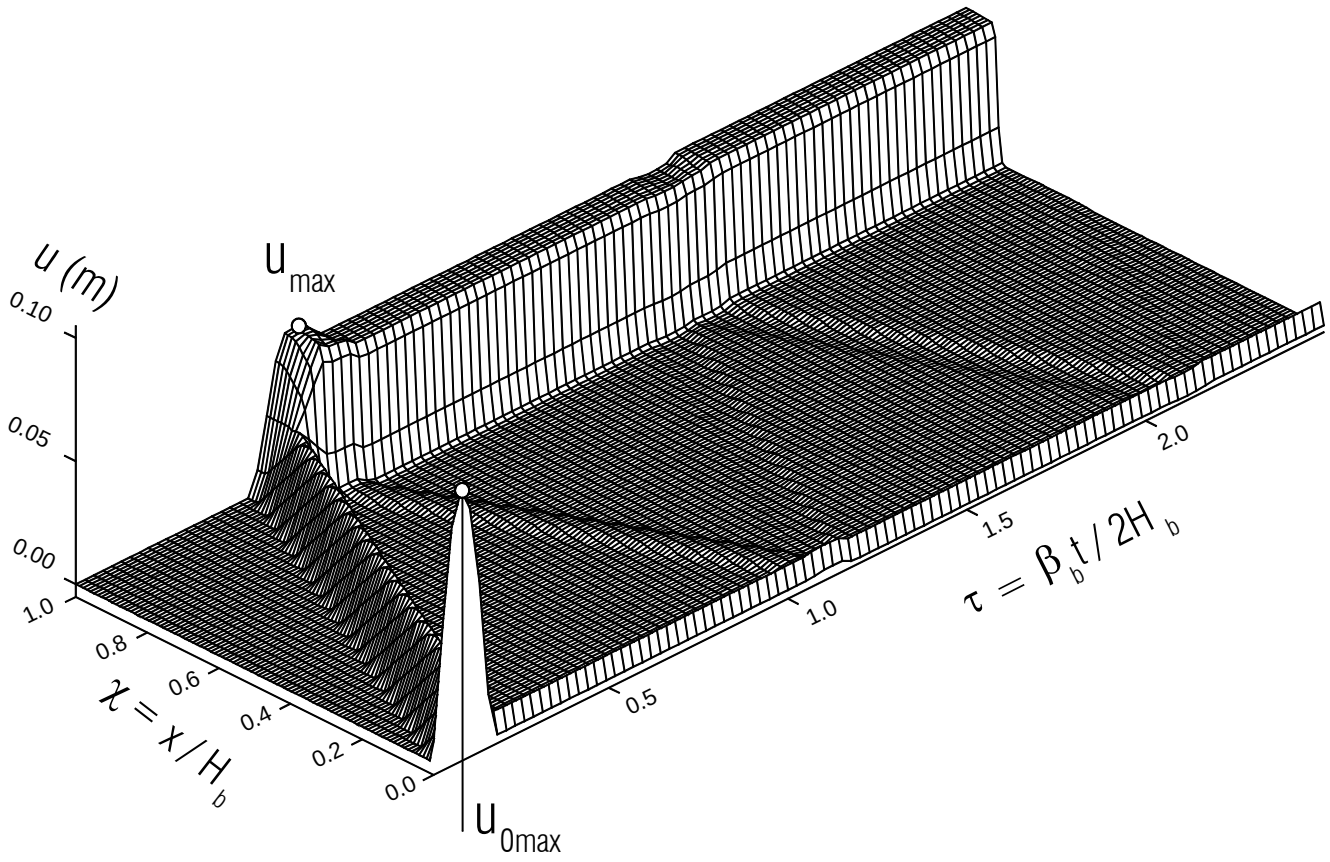
u (m)
0.10
0.05
0.00
u max
1.0
0.8
0.6
0.4
0.2
0.0
χ = x / H b
0.5
1.0
1.5
2.0
τ = β b t / 2H b
u 0max

Fig. 12a

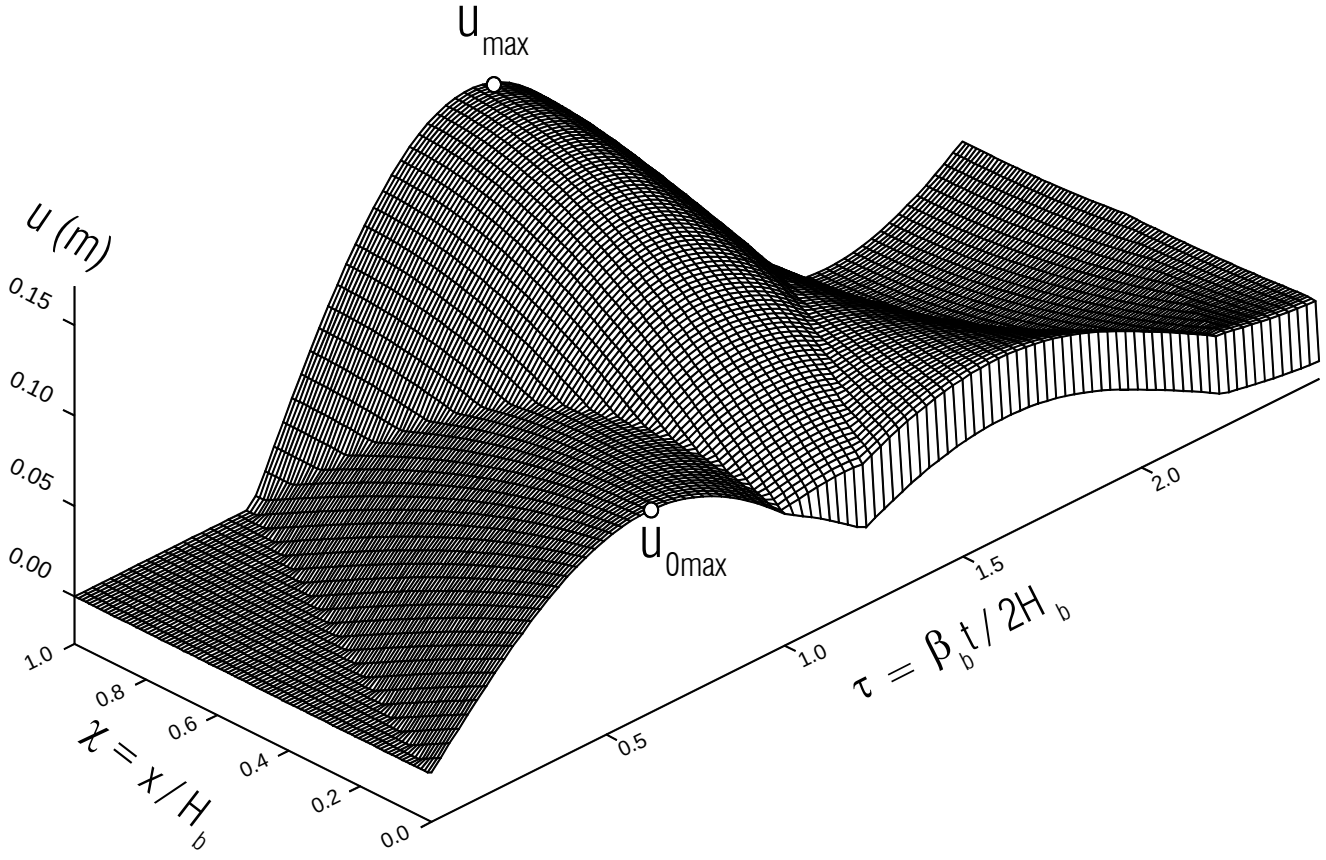
u_max
u_0max
u (m)
0.15
0.10
0.05
0.00
1.0
0.8
0.6
0.4
0.2
0.0
χ = x / H_b
0.5
1.0
1.5
2.0
τ = β_b t / 2H_b

Fig. 12b

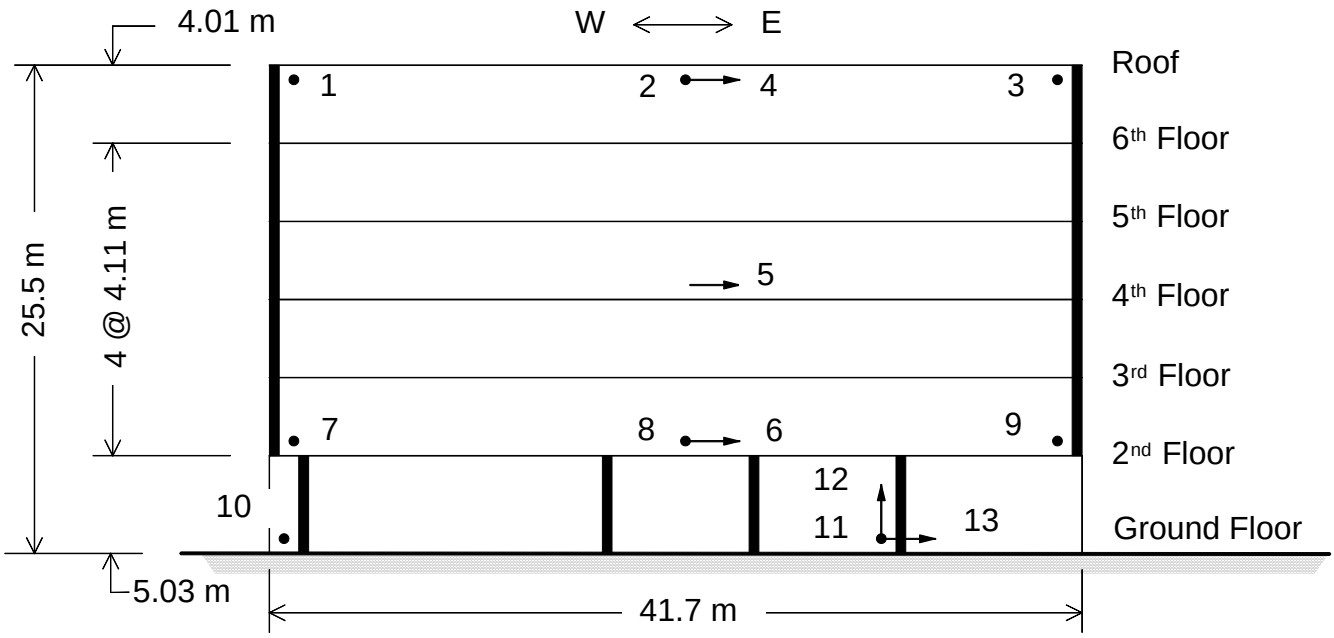
4.01 m
W
E
Roof
6th Floor
5th Floor
4th Floor
3rd Floor
2nd Floor
Ground Floor
1
2
4
3
5
7
8
6
9
10
12
11
13
25.5 m
4 @ 4.11 m
5.03 m
41.7 m

Fig. 13

NS motions

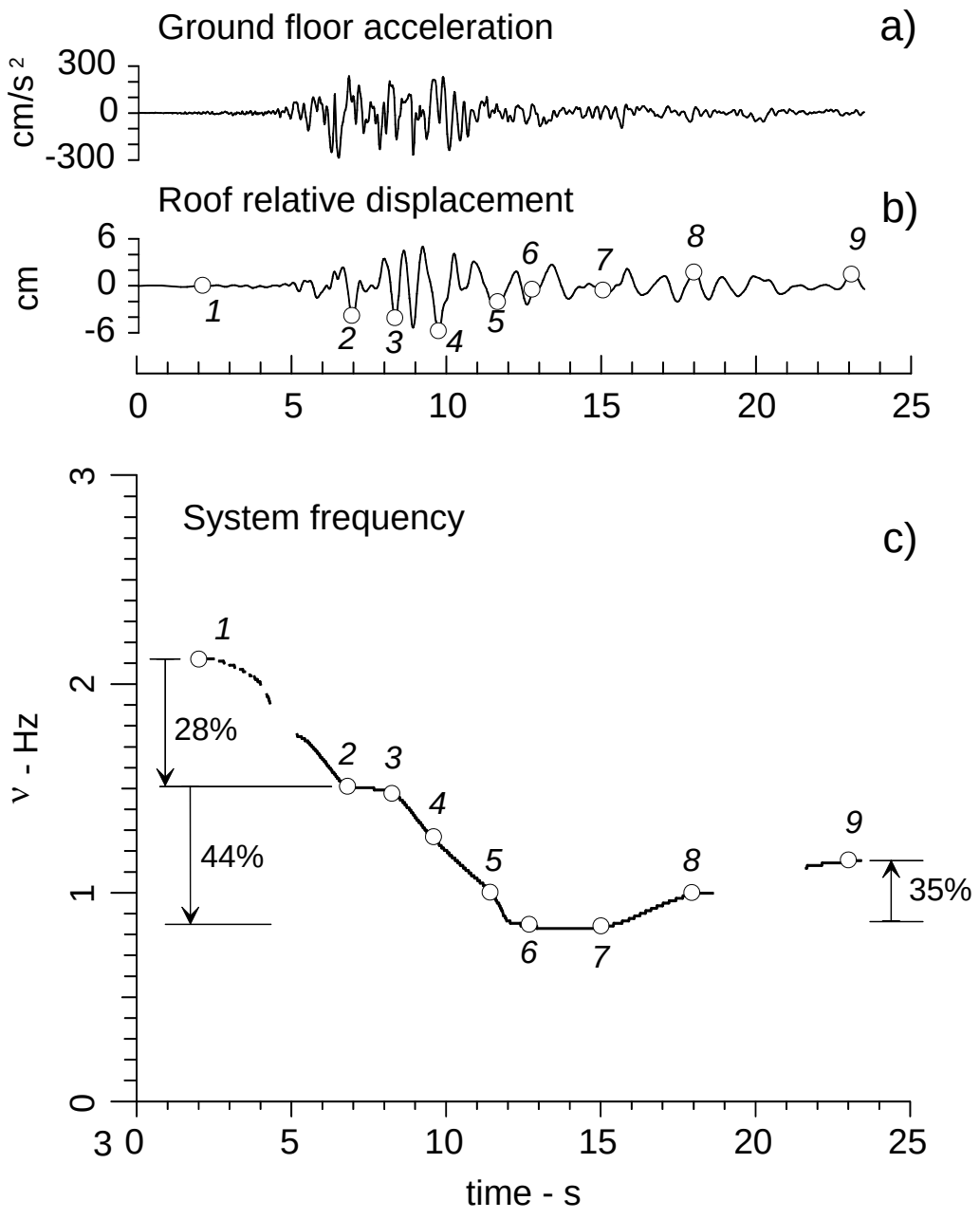

Fig. 14

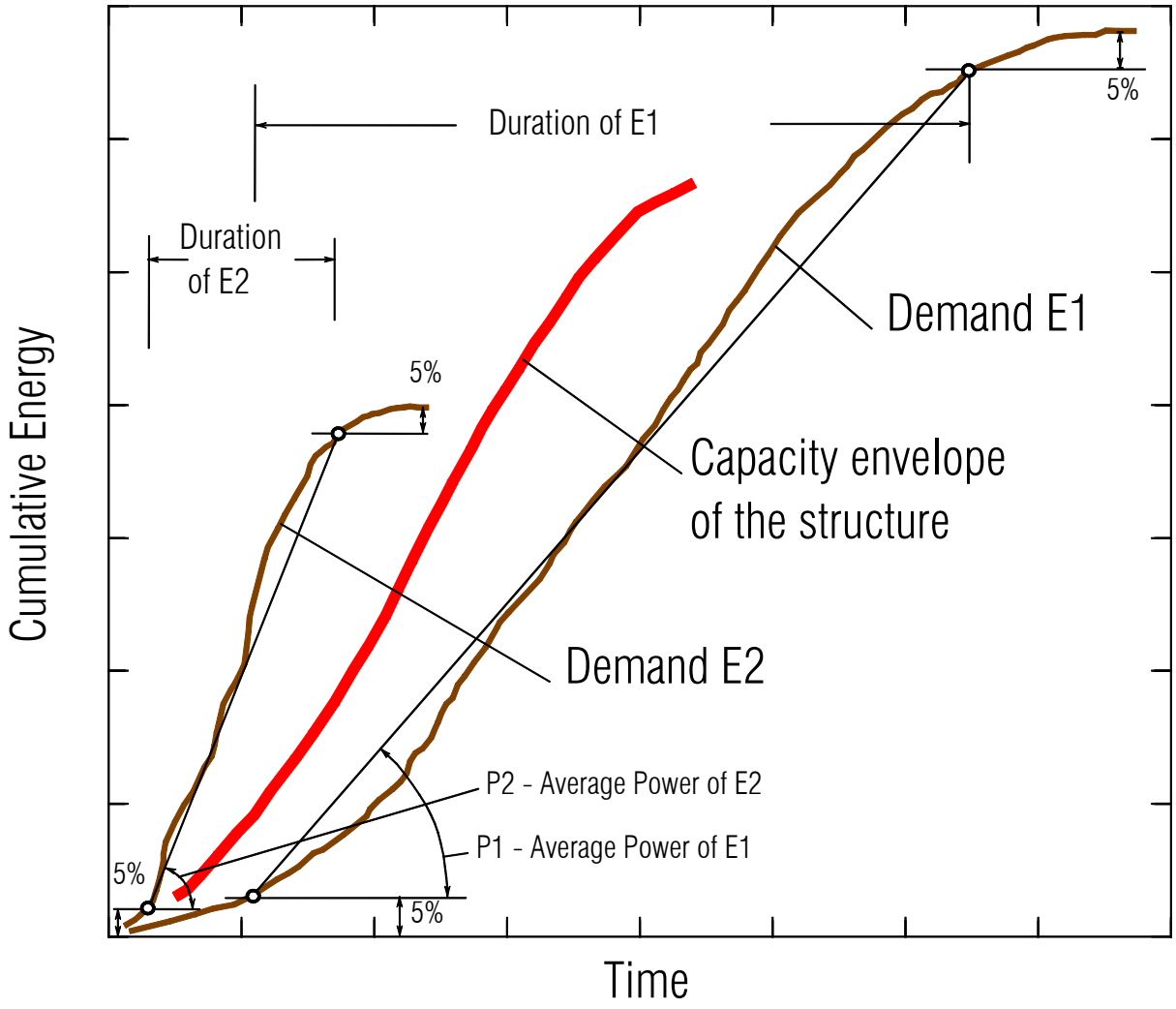
Cumulative Energy
Time
Duration of E1
Duration
of E2
5%
5%
Demand E1
Capacity envelope
of the structure
Demand E2
P2 - Average Power of E2
P1 - Average Power of E1
5%
5%

Fig. 15